

309

Two

MSC INTERNAL NOTE NO. 65-EG-58

PROJECT APOLLO

THE EFFECT OF VARIATIONS IN SPS ACTUATOR STIFFNESS ON
APOLLO THRUST VECTOR CONTROL SYSTEM STABILITY

Prepared by: Emery E. Smith, Jr.
Emery E. Smith, Jr.

Approved: David W. Gilbert
David W. Gilbert, Chief,
Engineering Simulation Branch

Approved: Robert G. Chilton
Robert G. Chilton, Deputy Chief,
Guidance and Control Division

NATIONAL AERONAUTICS AND SPACE ADMINISTRATION

MANNED SPACECRAFT CENTER

Houston, Texas

December 30, 1965

N70-76001

(ACCESSION NUMBER)

48

(PAGES)

TMX-65242

(NASA CR OR TMX OR AD NUMBER)

(THRU)

None

(CODE)

(CATEGORY)

SUMMARY

The Guidance and Control Division has conducted a linear, yaw-axis parameter study of SPS gimbal-actuator structural compliance effects on the SPS and SCS. The study shows that large changes in the actuator stiffness parameters, whether by way of increase or decrease, have little effect on the stability gain and phase margins of the system.

INTRODUCTION

The subject study is a followup of the reference study. It considers the effects of non-nominal actuator stiffness parameters on Apollo Block I thrust vector control system stability, whereas, the reference study considered nominal values only. The need to investigate non-nominal values of stiffness parameters was dictated by the lack of experimental verification of their actual values and the consequent lack of knowledge of their influence on SCS stability. The objectives of the study were: (1) to determine the stability gain and phase margins of the SPS and SCS as influenced by different actuator arm, mount, and gimbal stiffness values, and (2) to estimate the effect of these parameter changes on system time response.

SYSTEM DESCRIPTION

The Apollo autopilot or TVC system (exclusive of trim follower) is represented by the block diagrams of figures 1 and 2. Figure 2 is an expanded version of figure 1 obtained by reducing the equations (1 through 5) of figure 1. The positive root indicated in the forward loop transfer function (δ/T) of figure 2 is contributed by the "dog-wags-tail" (DWT) reaction and was not considered in the referenced study.

DISCUSSION OF RESULTS

The stiffness parameters, K_A , K_L , K_T (defined in the list of symbols) were varied individually and in combination. These variations are tabulated in Table II and referenced to the frequency response plots which show their effects. Figures 3 through 11 are the frequency response characteristics of the SPS; figures 12 through 20 are frequency response characteristics of the attitude rate loop of the SCS; and figures 21 through 29 are frequency response characteristics of the attitude position loop of the SCS. Gain and phase margins taken from these frequency response plots are summarized in Table III.

The frequency response characteristics of the SPS and SCS have an antiresonant peak. The antiresonance of the SPS is due to the actuator compliance and the frequency at which it occurs is a function of K_L and K_T . As K_L and K_T are varied, the frequency varies according to the definition: $\omega = \sqrt{1/\gamma_1}$, where γ_1 is defined in the list of symbol definitions. On the other hand, the antiresonance of the SCS is not a function of actuator compliance but is caused by the "tail-wags-dog" reaction, an inertial effect, and it occurs at the frequency

$$\omega = \sqrt{1/\gamma_7} = \sqrt{FD_X/J_X}.$$

Because "DWT" reaction was not included in the reference study, figures 30 through 34 have been added here so that the frequency response characteristics of the nominal system may be compared with the reference study. The frequency response characteristic of the SPS tachometer loop, shown in figure 30, exhibits the instability caused by the DWT reaction. Mathematically, the possibility of this instability occurring is indicated by the positive root in the characteristic equation (δ/T), which expresses the positive feedback on δ of the DWT (ψ) term of equation 2. This tachometer loop instability is not detrimental to operations because the overall SPS closed loop system has adequate gain and phase margins as indicated by figure 3.

To estimate the effects of the stiffness parameter variations on system time response, the poles of the closed loop systems (SPS, attitude rate of SCS, and attitude position of SCS) were plotted for each stiffness parameter condition. Figures 35, 36, and 37 are plots of the low frequency poles ($\omega < 30$ rad/sec) of the SPS, attitude rate of the SCS, and attitude position of the SCS, respectively. The high frequency poles are of little consequence to the time response as their contribution is greatly attenuated by the system. The plots show that as stiffness is reduced, the poles move toward the origin lowering system damping and natural frequency. Conversely, increasing stiffness increases the damping and natural frequency of the system.

CONCLUSIONS

Lowering the gimbal-actuator assembly stiffness reduces (1) the gain and phase margins of the overall SPS and (2) the gain margin of the attitude rate loop of the SCS. The phase margin of the attitude position loop were only slightly affected. Increasing the stiffness tended to improve the stability margins.

To a first approximation, the low frequency poles indicate that reducing stiffness values causes settling time to increase due to lowered damping and natural frequency. It should be noted that the closed loop time response of the SCS will change very little because the controlling pole remains approximately stationary when the stiffness is lowered. The data also indicate that the time response will improve slightly for an increase in stiffness.

SYMBOL DEFINITION

D_e	- Distance from engine gimbal to engine c.m. along the engine center line; ft
D_x	- Distance from engine gimbal to system c.m. along the body x-axis; ft
F	- Engine thrust; lbs
I_{zz}	- Moment of inertia of system about c.m.; lb-ft-sec ²
I_c	- Actuator clutch current; amps
J_a	- Moment of inertia of bull gear and clutch reflected to bull gear; lb-ft-sec ²
J_n	- Nozzle moment of inertia about engine c.m.; lb-ft-sec ²
K_a	- Actuator arm stiffness; lb/ft
K_c	- Forward loop gain constant; N.D.
K_L	- Gimbal stiffness; lb/ft
K_T	- Actuator mount stiffness; lb/ft
K_e	- Actuator servo amplifier gain; amp/rad
K_γ	- Clutch gain; ft-lb/amp
K_ξ	- Actuation system rate feedback gain constant; rad/rad/sec
K_δ	- Actuation system nozzle position feedback gain constant; N.D.
$K_{\dot{\psi}}$	- SCS rate gyro feedback gain constant; rad/rad/sec
K_ψ	- SCS attitude gain constant; N.D.
M_E	- Engine mass; slugs
N	- Pitch of screw jack; rad/ft
$N^2 B_\theta$	- Total damping of actuator lumped tachometer, reflected to engine; lb-sec/ft
R	- Actuator lever arm; ft
S	- LaPlacian operator; "sec ⁻¹ "

SYMBOL DEFINITION (Continued)

T	- Clutch torque; ft-lb
x_2	- Actuator mount deflection; ft
δ	- Gimbal position; rad
δ_c	- Gimbal position command; rad
δ_{po}	- Pickoff position; radians of gimbal deflection
δ_T	- Tachometer position; rad
ψ	- Attitude position; rad
G	- Gain; decibels
G_m	- Gain margin $\equiv -G @ \omega_\phi$; decibel
ϕ	- Phase angle; degs
ϕ_{pm}	- Phase margin $\equiv 180^\circ - \phi @ \omega_c$; degs
ω_ϕ	- Frequency where $\phi = 180^\circ$; rad/sec
ω_c	- Frequency where $G = 0\text{db}$; rad/sec
J_x	$= J_n + M_e D_e D_x$
C_1	$= K_L K_T R^2 / J_n$
C_2	$= C_1 - (K_T + K_L) (J_x / J_n) (FD_x / I)$
C_3	$= K_A / (K_T (K_A + K_L) + K_A K_L)$
C_4	$= C_1 C_3 - (J_x / J_n) (FD_x / I)$
C_5	$= C_3 (J_x / J_n) (FD_x / I) (K_L K_T / N^2 J_A)$
C_6	$= (1 - J_x^2 / J_n I)$
C_7	$= (FD_x / I)$
γ_1	$= (K_T + K_L) (C_y / C_2)$
γ_2	$= C_6 / C_4$
γ_3	$= C_6 / C_5$

SYMBOL DEFINITION (Continued)

$$\gamma_4 = (N^2 B_\theta) / N^2 J_A \quad (C_5 / C_5)$$

$$\gamma_5 = [C_4 + C_3 C_6 (K_T K_L / N^2 J_A)] / C_5$$

$$\gamma_6 = (N^2 B_\theta / N^2 J_A) \quad (C_4 / C_5)$$

$$\gamma_7 = (J_X / F D_X)$$

REFERENCE

1. MSC Internal Note No. 65-EG-42, "A Linear, Single-Plane Study of the Effect of SPS Actuator Compliance on the Response Characteristics of the Apollo Block I SCS, September 29, 1965

TABLE I

Constants

<u>Quantity</u>	<u>Value</u>	<u>Units</u>
D_e	.667	Ft.
D_x	9.62	Ft.
F	21900.	Lbs.
I_{zz}	52400.	Ft-lb-sec ²
J_a	$70/(96 \pi)^2$	Ft-lb-sec ²
J_n	220	Ft-lb-sec ²
K_{a_c}	1.2×10^6	Lb/ft
K_c	1.5	N.D.
K_{L_c}	2.0×10^6	Lb/ft
K_{T_c}	$.576 \times 10^6$	Lb/ft
K_E	20	amps/rad
K_r	3530	Ft-lb/amp
K_{δ}°	.09	rad/rad/sec
K_{δ}	1.0	N.D.
K_{φ}°	.5	rad/rad/sec
K_{φ}	1.0	N.D.
M_E	20	Slugs
N	96π	rad/ft
$N^2 B_{\theta}$	2000	lb-sec/ft
R	1.	Ft.

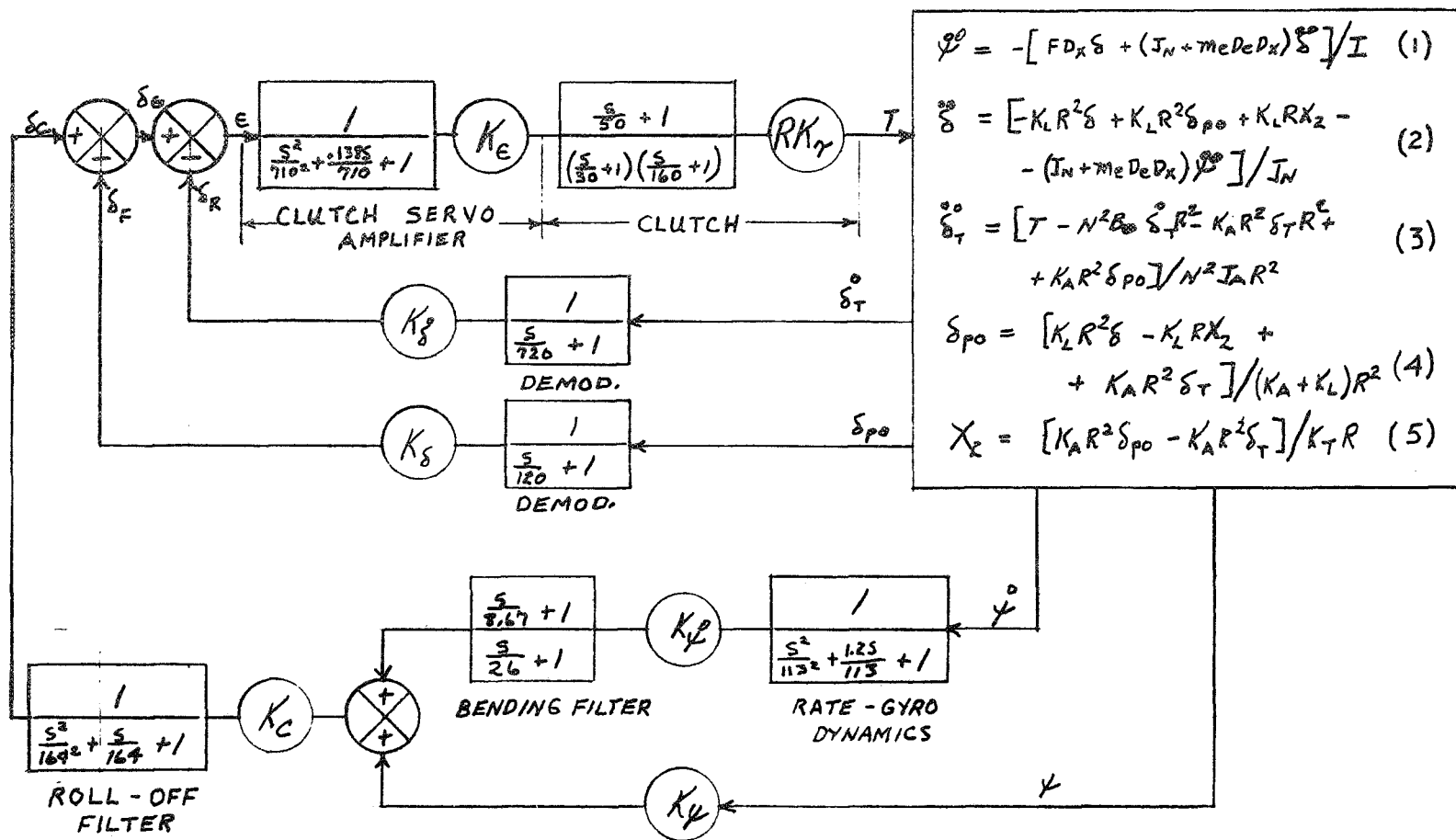
TABLE II
STIFFNESS PARAMETER CONDITIONS CORRESPONDING TO THE FREQUENCY
RESPONSE CHARACTERISTICS SHOWN IN FIGURES 3 TO 34

Figure No.	Configuration	Transfer Function	K_A	K_L	K_T
3	SPS Position Loop, Open	δ_F / δ_e	NOM	NOM	NOM
4	"	"	"	"	$\frac{1}{2}$ NOM
5	"	"	"	$\frac{1}{2}$ NOM	NOM
6	"	"	$\frac{1}{2}$ NOM	NOM	"
7	"	"	"	$\frac{1}{2}$ NOM	$\frac{1}{2}$ NOM
8	"	"	$\frac{1}{4}$ NOM	$\frac{1}{4}$ NOM	$\frac{1}{4}$ NOM
9	"	"	NOM	NOM	2 NOM
10	"	"	"	2 NOM	NOM
11	"	"	2 NOM	NOM	"
12	SCS Rate Loop, Open	γ_R / δ_c	NOM	NOM	NOM
13	"	"	"	"	$\frac{1}{2}$ NOM
14	"	"	"	$\frac{1}{2}$ NOM	NOM
15	"	"	$\frac{1}{2}$ NOM	NOM	"
16	"	"	"	$\frac{1}{2}$ NOM	$\frac{1}{2}$ NOM
17	"	"	$\frac{1}{4}$ NOM	$\frac{1}{4}$ NOM	$\frac{1}{4}$ NOM
18	"	"	NOM	NOM	2 NOM
19	"	"	"	2 NOM	NOM
20	"	"	2 NOM	NOM	"
21	SCS Position Loop, Open	γ_F / γ_e	NOM	NOM	NOM
22	"	"	"	"	$\frac{1}{2}$ NOM
23	"	"	"	$\frac{1}{2}$ NOM	NOM
24	"	"	$\frac{1}{2}$ NOM	NOM	"
25	"	"	"	$\frac{1}{2}$ NOM	$\frac{1}{2}$ NOM
26	"	"	$\frac{1}{4}$ NOM	$\frac{1}{4}$ NOM	$\frac{1}{4}$ NOM
27	"	"	NOM	NOM	2 NOM
28	"	"	"	2 NOM	NOM
29	"	"	2 NOM	NOM	"
30	SPS Rate Loop, Open	δ_R / ϵ	NOM	NOM	NOM
31	SPS Rate Loop, Closed	δ_R / δ_e	"	"	"
32	SPS Position Loop, Closed	δ_F / δ_c	"	"	"
33	SCS Rate Loop, Closed	γ_R / γ_e	"	"	"
34	SCS Position Loop, Closed	γ_F / γ_c	"	"	"

TABLE III

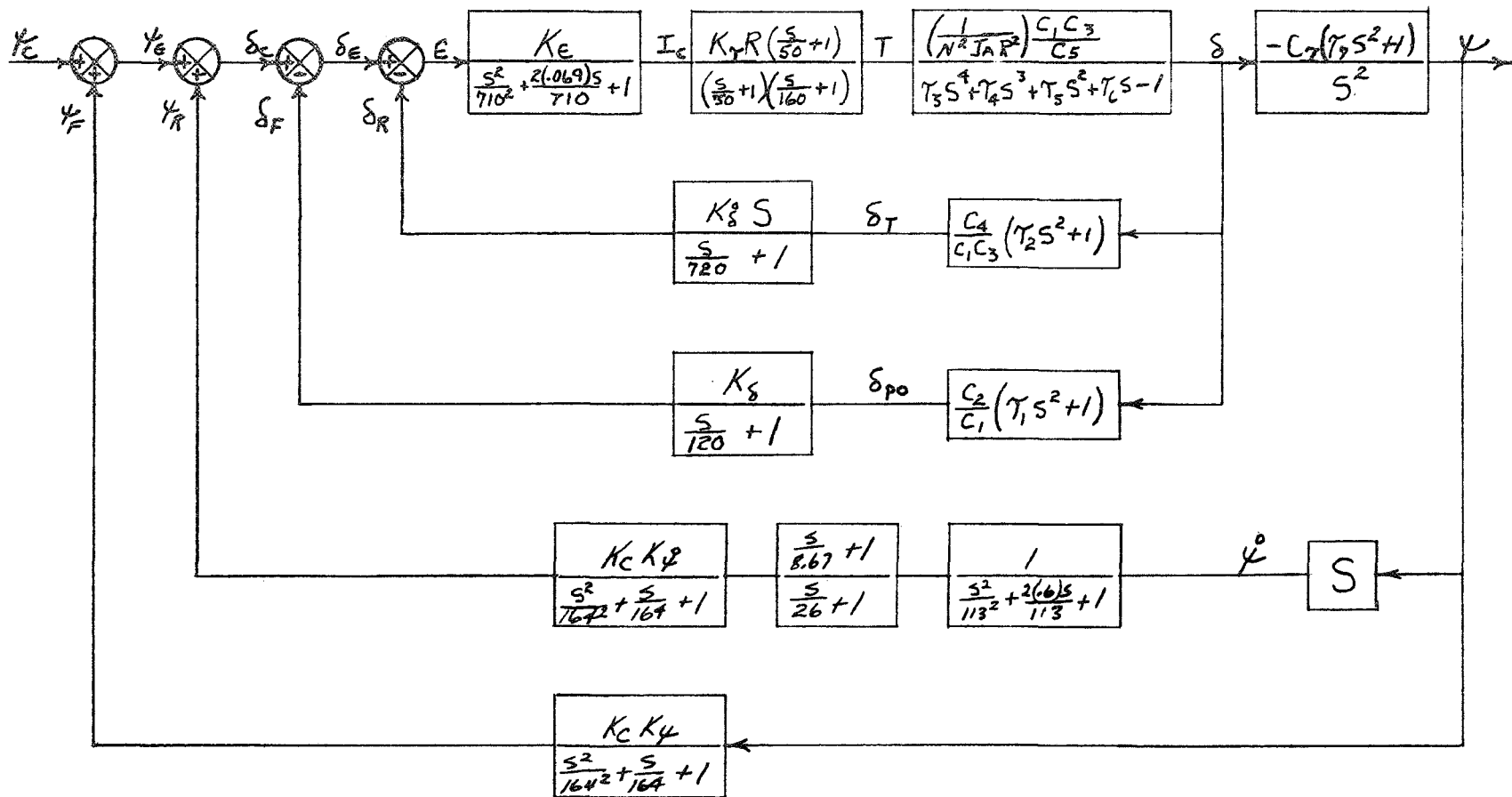
*Stiffness Parameter Condition	SPS		SCS			
			Attitude Rate Loop		Attitude Position Loop	
	$(G_m(\text{db} @ \omega_\phi))$	$\phi_{pm}(\text{deg} @ \omega_c)$	$G_m(\text{db} @ \omega_\phi)$	$\phi_{pm}(\text{deg} @ \omega_c)$	$G_m(\text{db} @ \omega_\phi)$	$\phi_{pm}(\text{deg} @ \omega_c)$
All Nominal	13. @ 25.	65. @ 15.	16. @ 15.	80. @ 3.	12.5 @ 5.3	50. @ 1.8
$K_T = \frac{1}{2}$ NOM	13. @ 22.	65. @ 8.	15. @ 15.	80. @ 3.	13. @ 5.3	50. @ 1.8
$K_L = \frac{1}{2}$ NOM	12.5 @ 24.	65. @ 8.	16. @ 16.	80. @ 3.	13. @ 5.4	50. @ 1.8
$K_A = \frac{1}{2}$ NOM	11. @ 24.	64. @ 8.	16. @ 16.	80. @ 3.	13. @ 5.5	50. @ 1.8
All $K = \frac{1}{2}$ NOM	10. @ 21.	64. @ 8.	12. @ 15.	80. @ 3.	13. @ 5.5	50. @ 1.8
All $K = \frac{1}{4}$ NOM	8. @ 17.	61. @ 9.	6.8 @ 13.5	80 @ 3.	13. @ 5.5	50. @ 1.8
$K_T = 2$ NOM	13. @ 26.	65. @ 8.	18. @ 17.	80. @ 3.	14. @ 5.5	50. @ 1.8
$K_L = 2$ NOM	13. @ 25.	65. @ 8.	17. @ 16.	80. @ 3.	13. @ 5.5	50. @ 1.8
$K_A = 2$ NOM	13. @ 26	65. @ 8.	17. @ 16.	80. @ 3.	13. @ 5.5	50. @ 1.8

*Each parameter nominal unless otherwise noted.



AUTOPILOT

FIGURE 1



AUTOPILOT

FIGURE 2

Frequency Response
SPS Position Loop Open
($\delta F/\delta C$) - Nominal

00000000

BODE PLOT

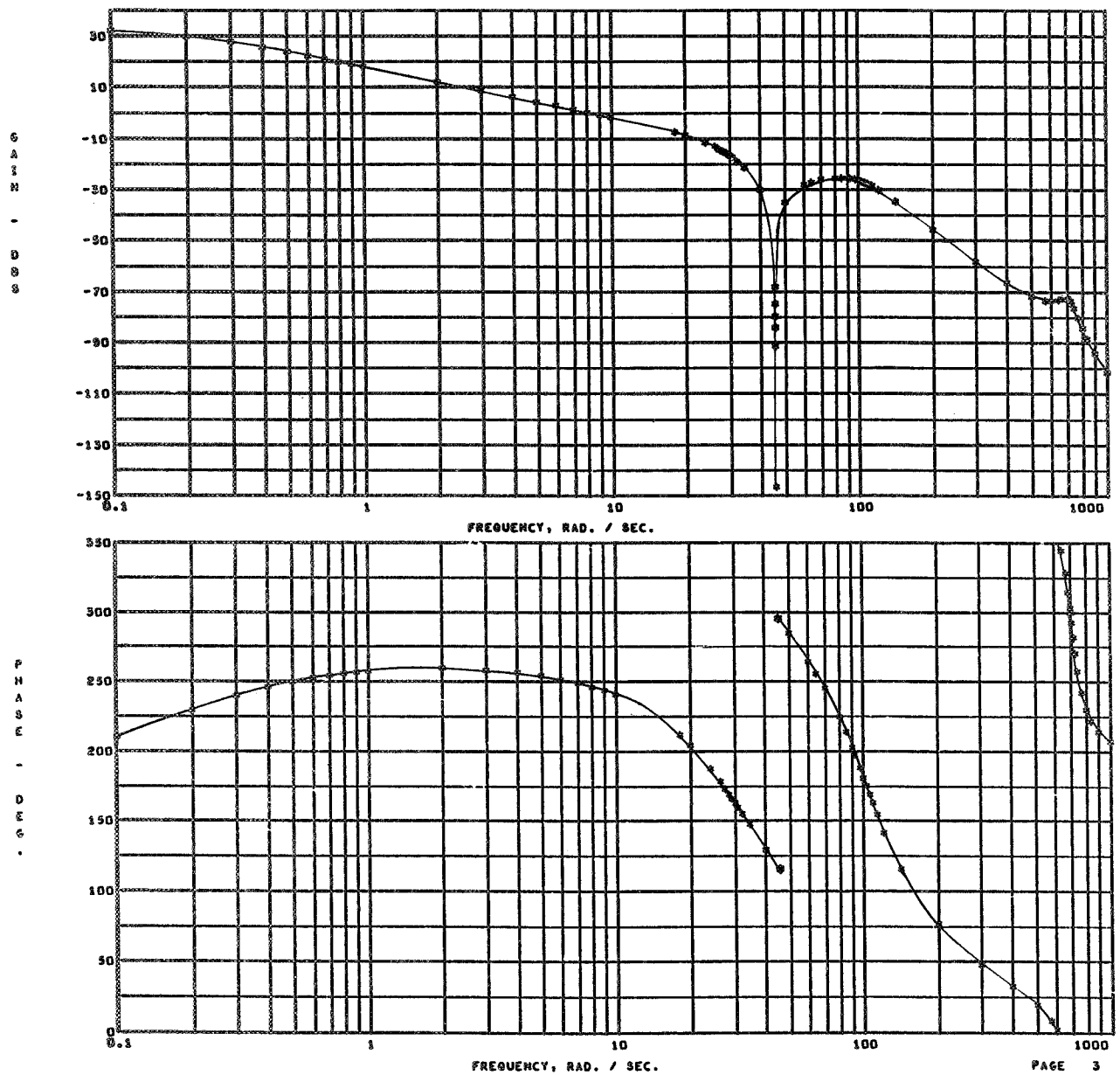
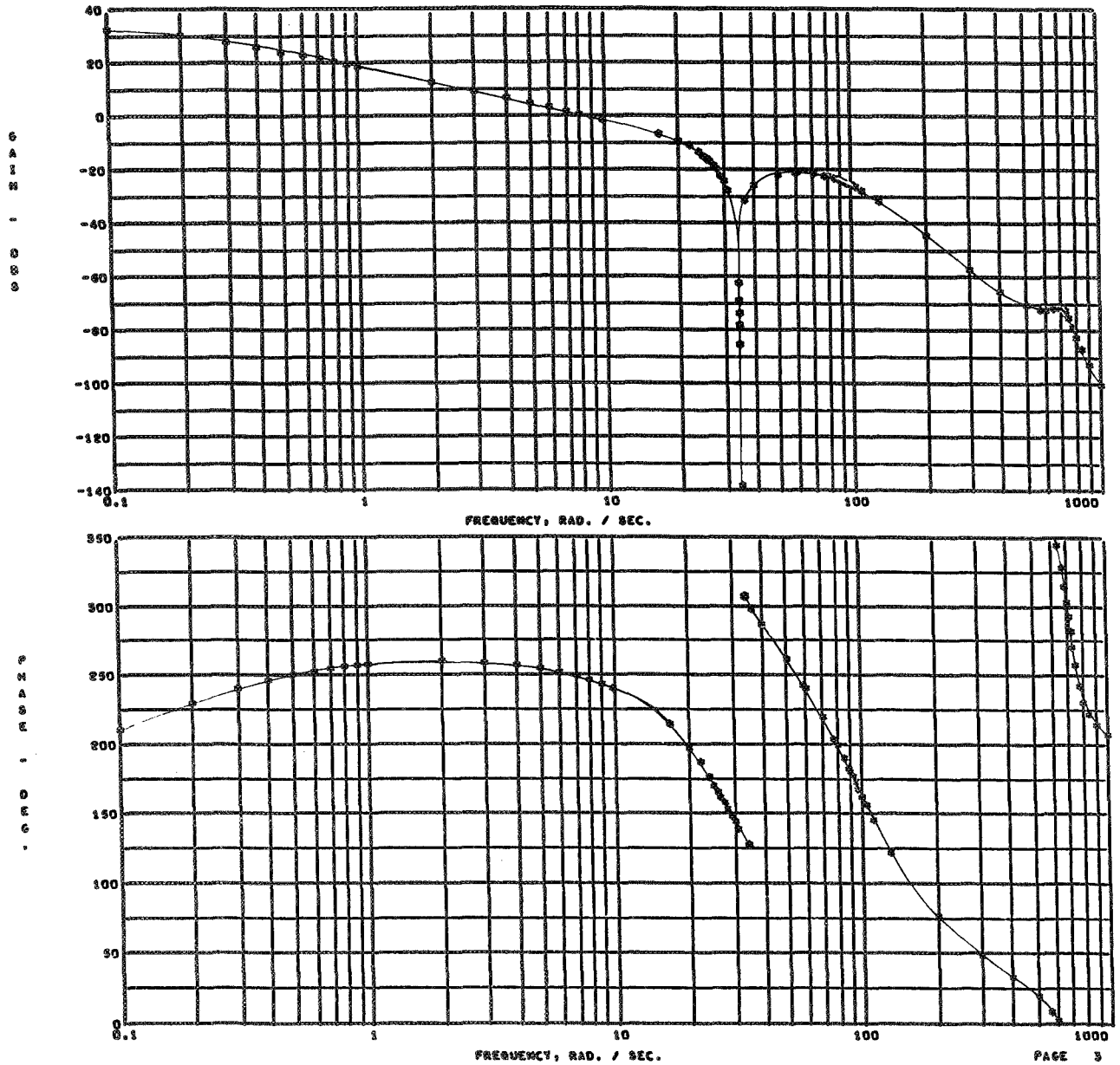


Figure 3

Frequency Response
 SPS Position Loop Open
 $(\delta F / \delta \epsilon) - K_T = 1/2 \text{ Nom}$

00000000

BODE PLOT



FREQUENCY, RAD. / SEC.

PAGE 3

Figure 4

Frequency Response
SPS Position Loop Open
($\delta F / \delta \epsilon$) - $K_L = 1/2$ Nom

00000000

BODE PLOT

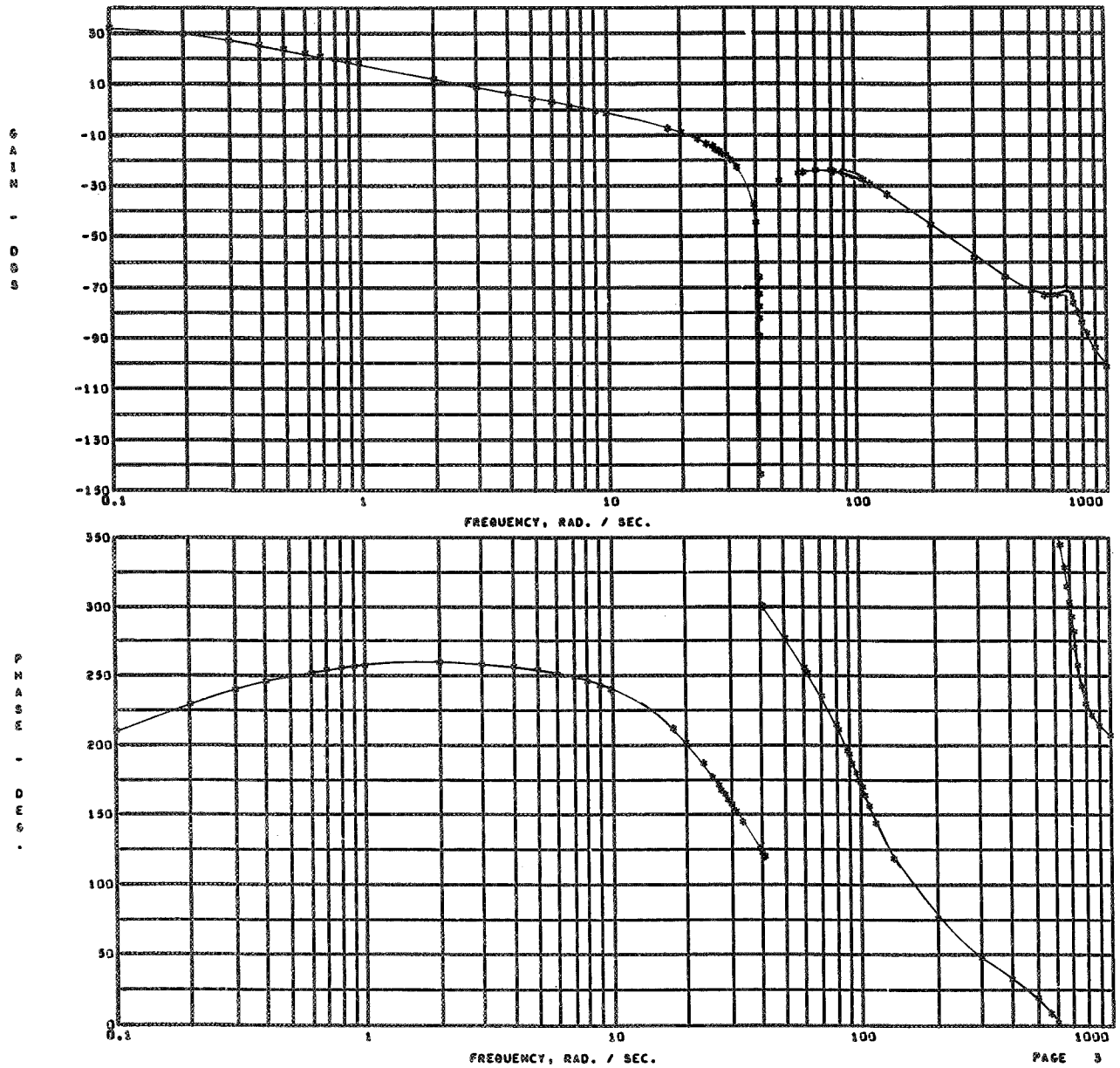
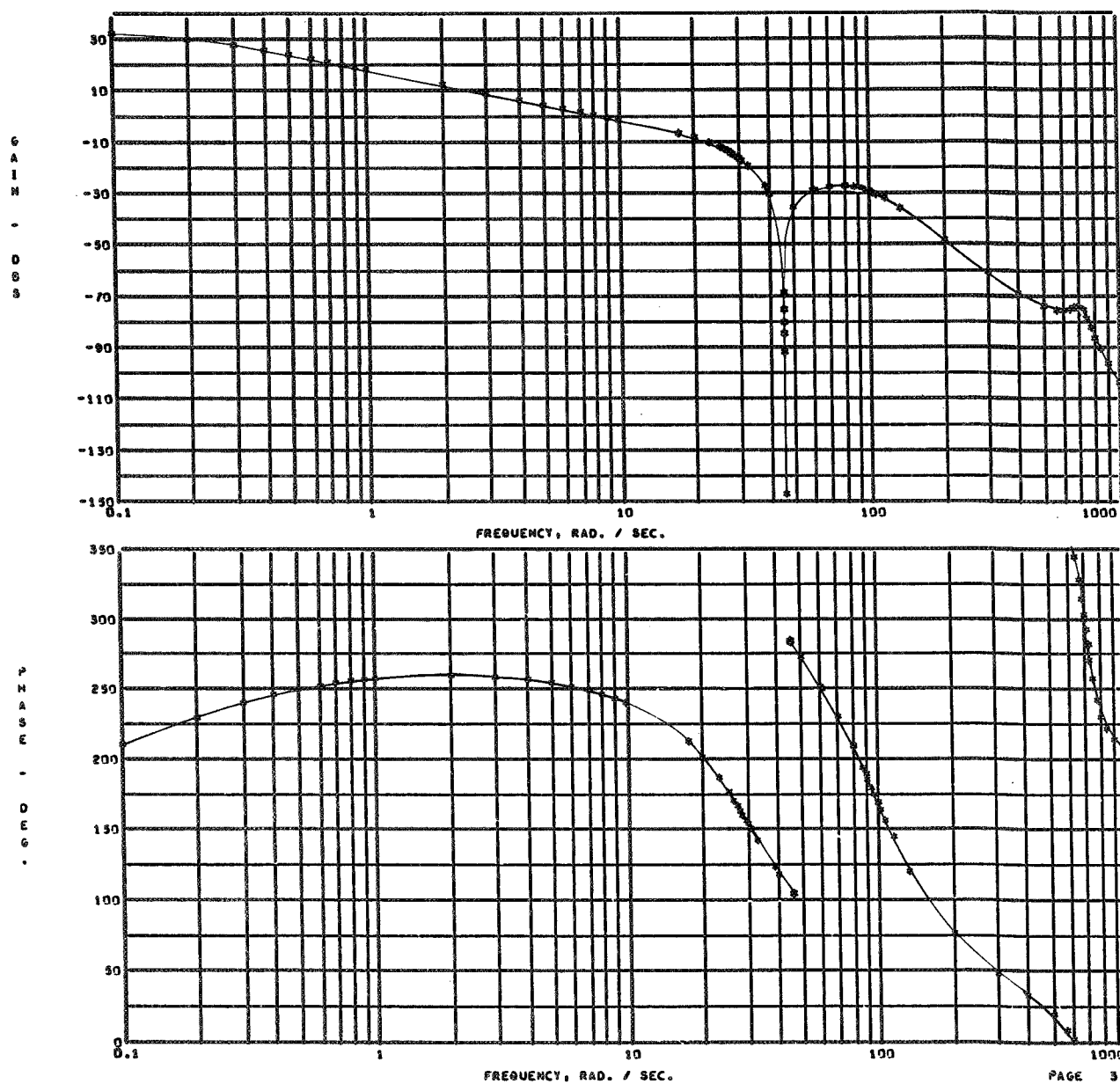


Figure 5

Frequency Response
 SPS Position Loop Open
 $(\delta F / \delta \epsilon) - K_A = 1/2 \text{ Nom}$

00000000

BODE PLOT



FREQUENCY, RAD. / SEC.

PAGE 3

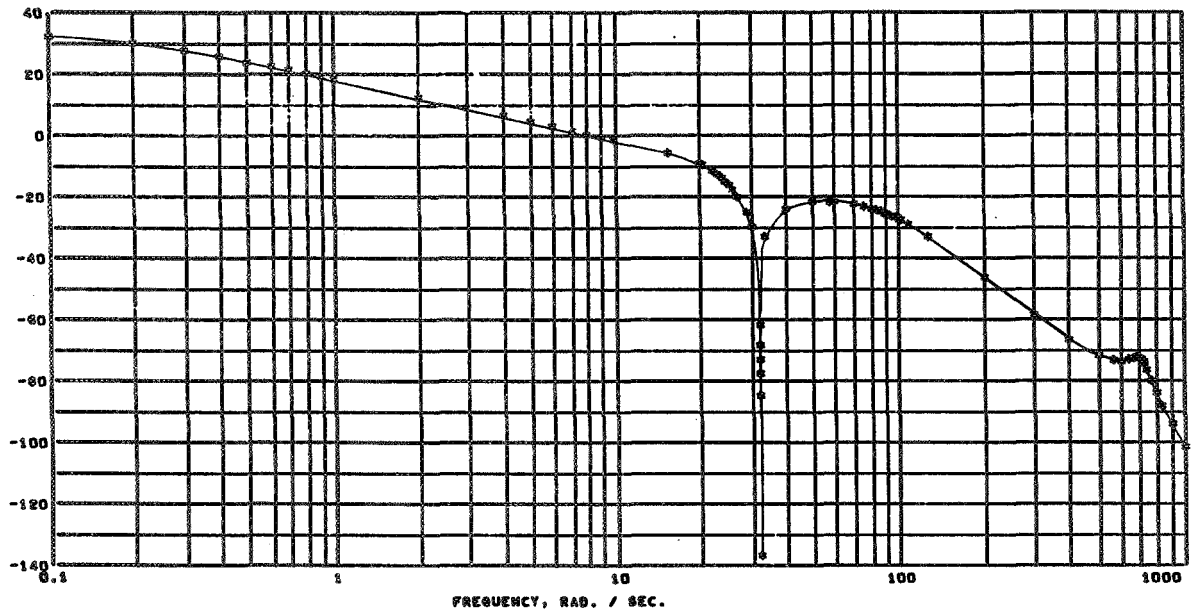
Figure 6

Frequency Response
SPS Position Loop Open
($\delta F / \delta \epsilon$) - All: 1/2 Nom

BODE PLOT

00000000

GAIN



PHASE

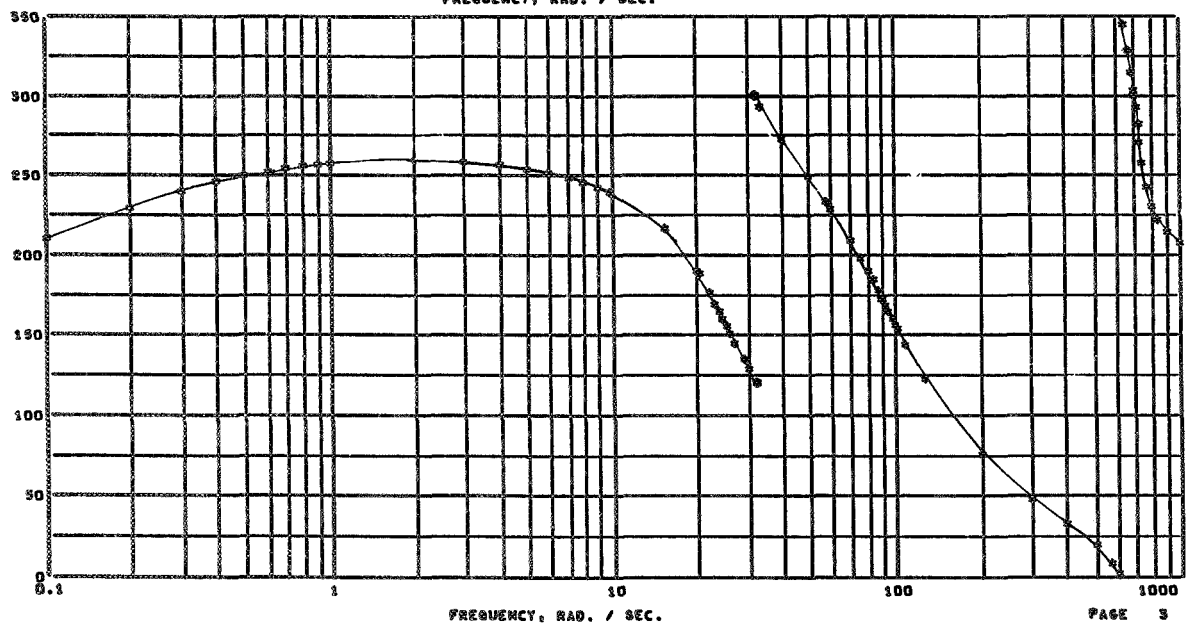


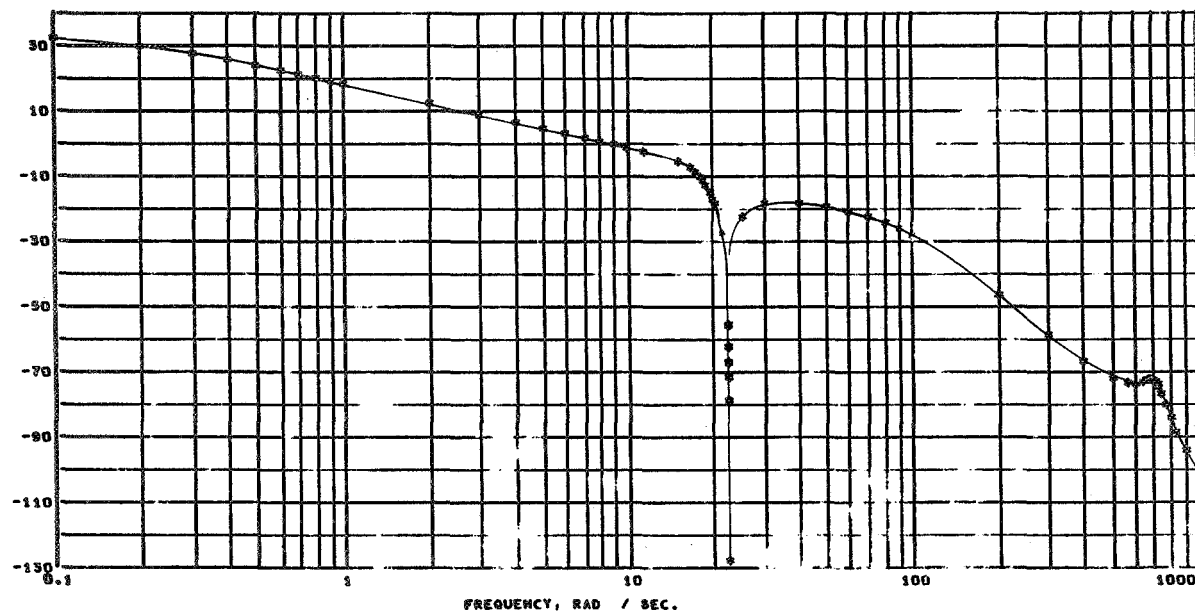
Figure 7

Frequency Response
SPS Position Loop Open
($\delta F / \delta \epsilon$) - All: 1/4 Nom

00000000

BODE PLOT

G
A
I
N
-
D
B
S



P
H
A
S
E
-
D
E
G
.

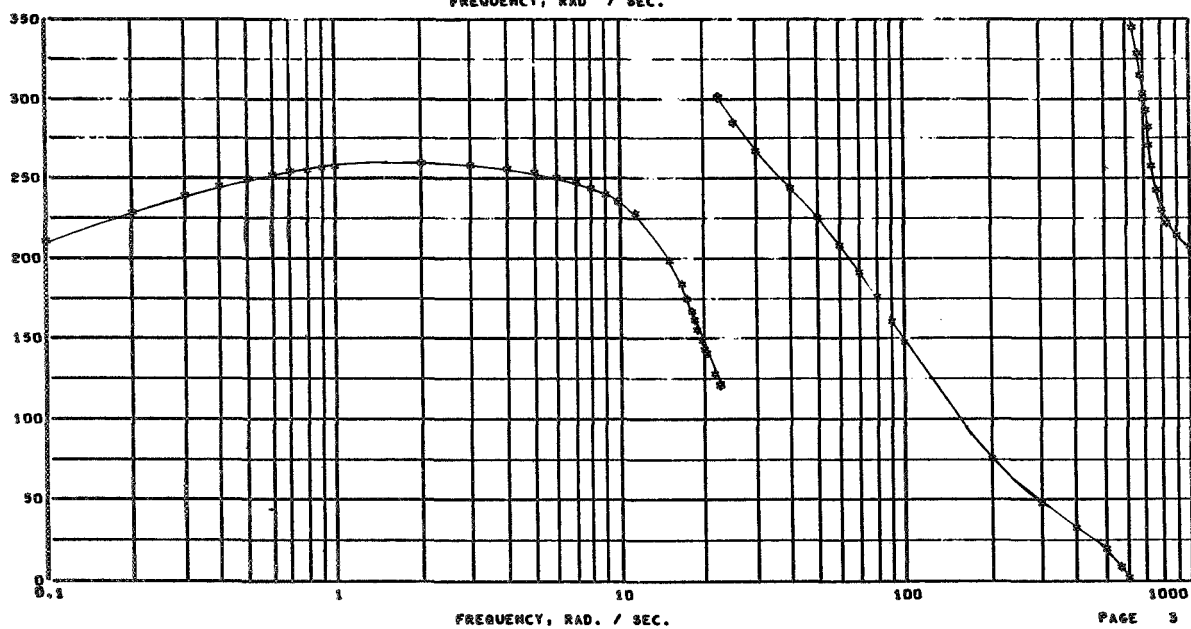


Figure 8

Frequency Response
 SPS Position Loop Open
 $(\delta F / \delta \epsilon) - K_T = 2 \text{ Nom}$

00000000

BODE PLOT

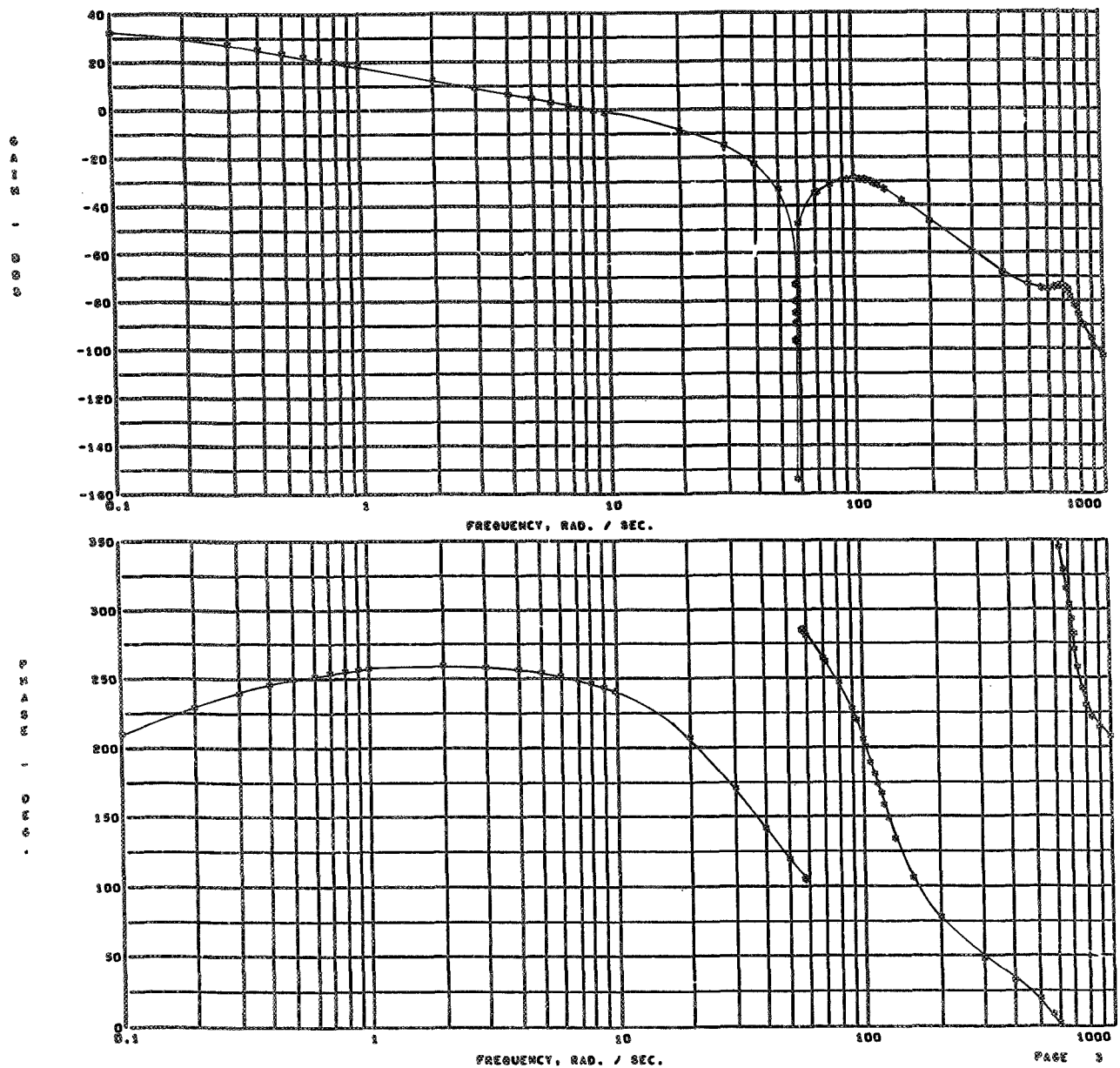


Figure 9

Frequency Response
SPS Position Loop Open
 $(\delta F / \delta \epsilon) - K_L = 2 \text{ Nom}$

00000000

BODE PLOT

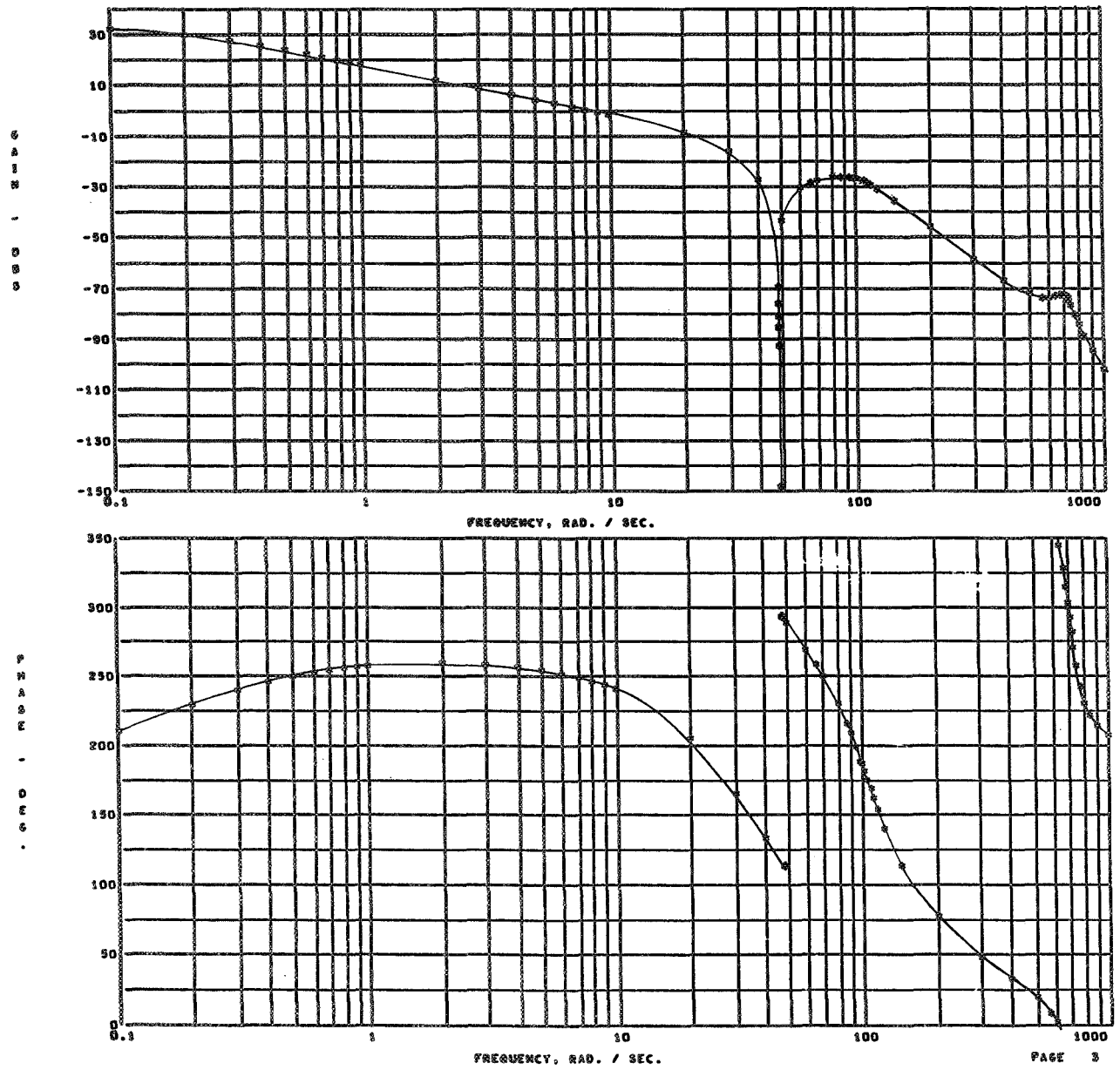


Figure 10

Frequency Response
SPS Position Loop Open
 $(\delta F / \delta e) - K_A = 2 \text{ Nom}$

00000000

BODE PLOT

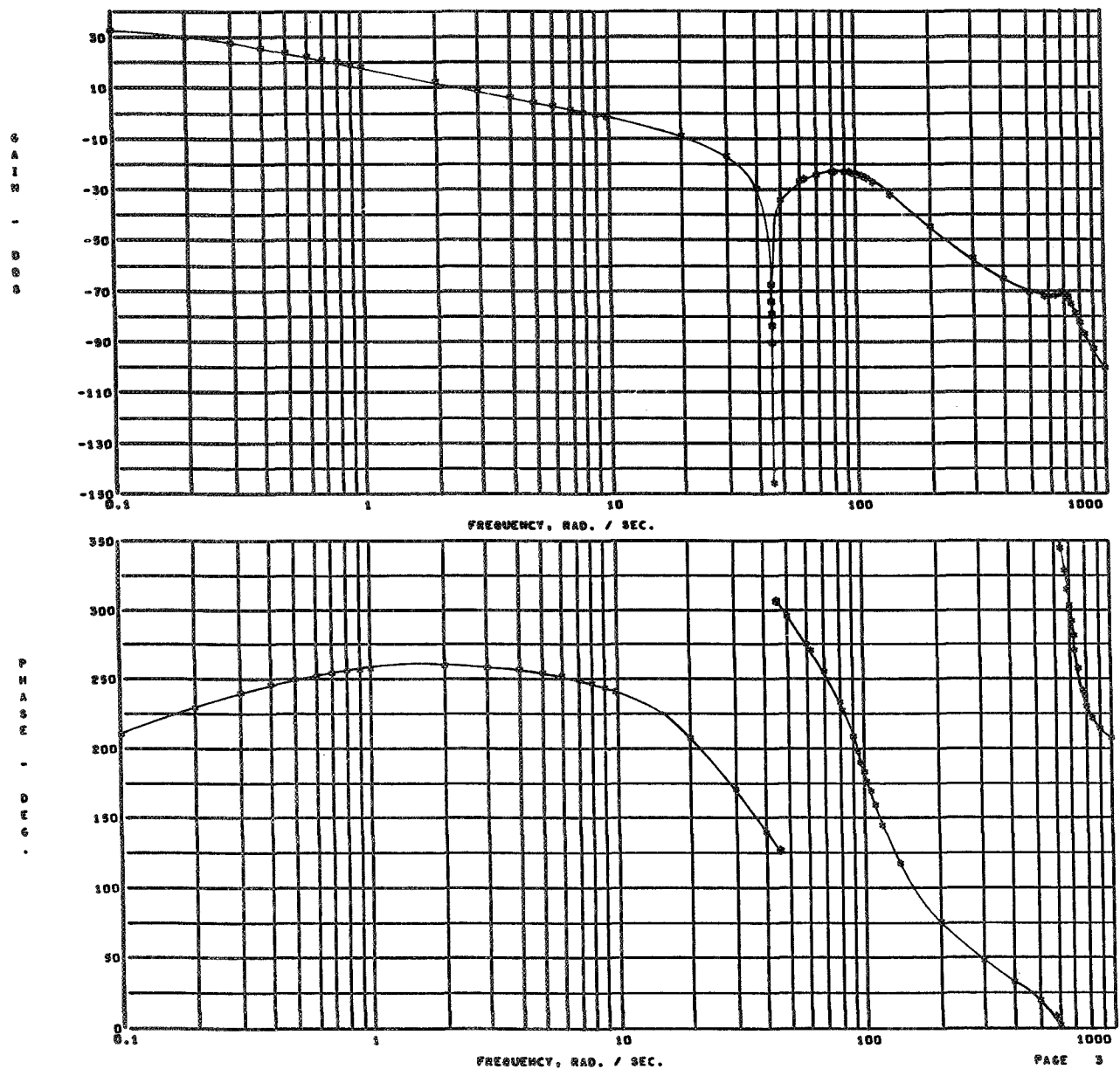


Figure 11

Frequency Response
SCS Rate Loop Open
(γ_R/δ_C) - Nominal

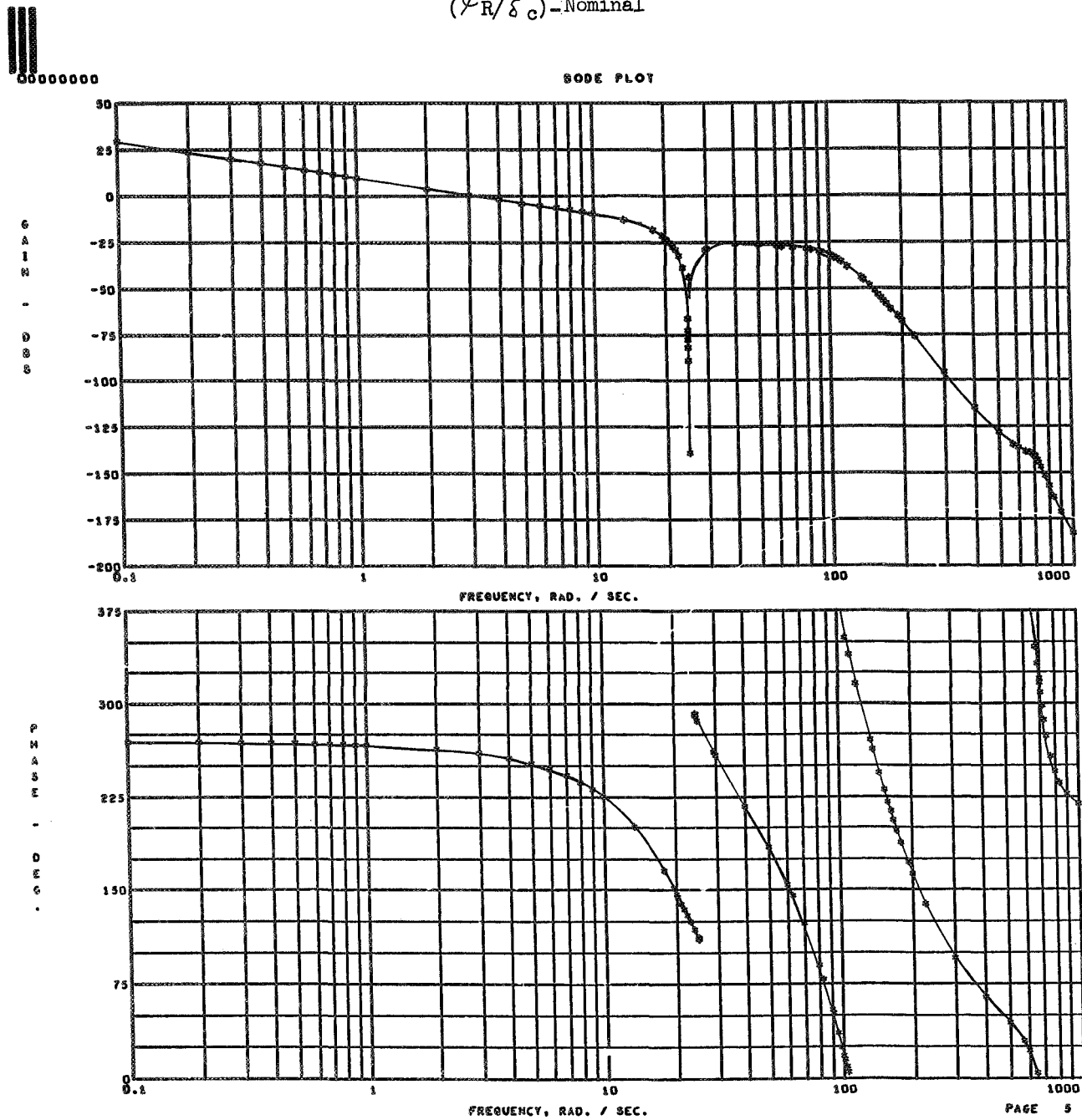


Figure 12

Frequency Response
SCS Rate Loop Open
 $(\psi R/\delta_C) - K_T = 1/2$ Nom



00000000

BODE PLOT

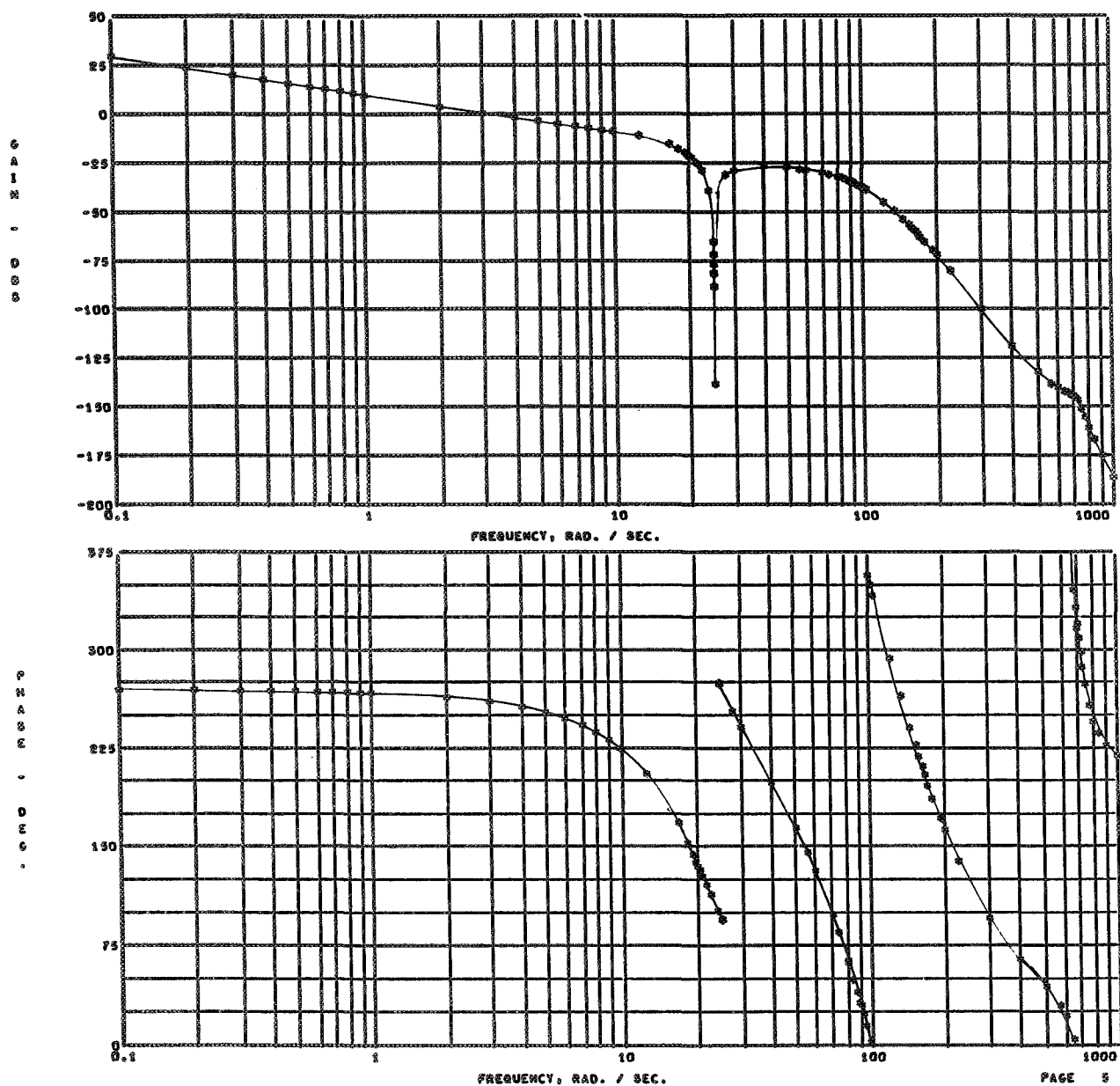


Figure 13

Frequency Response
SCS Rate Loop Open
 $(\varphi_R/\delta_c) - K_L = 1/2 \text{ Nom}$

00000000

BODE PLOT

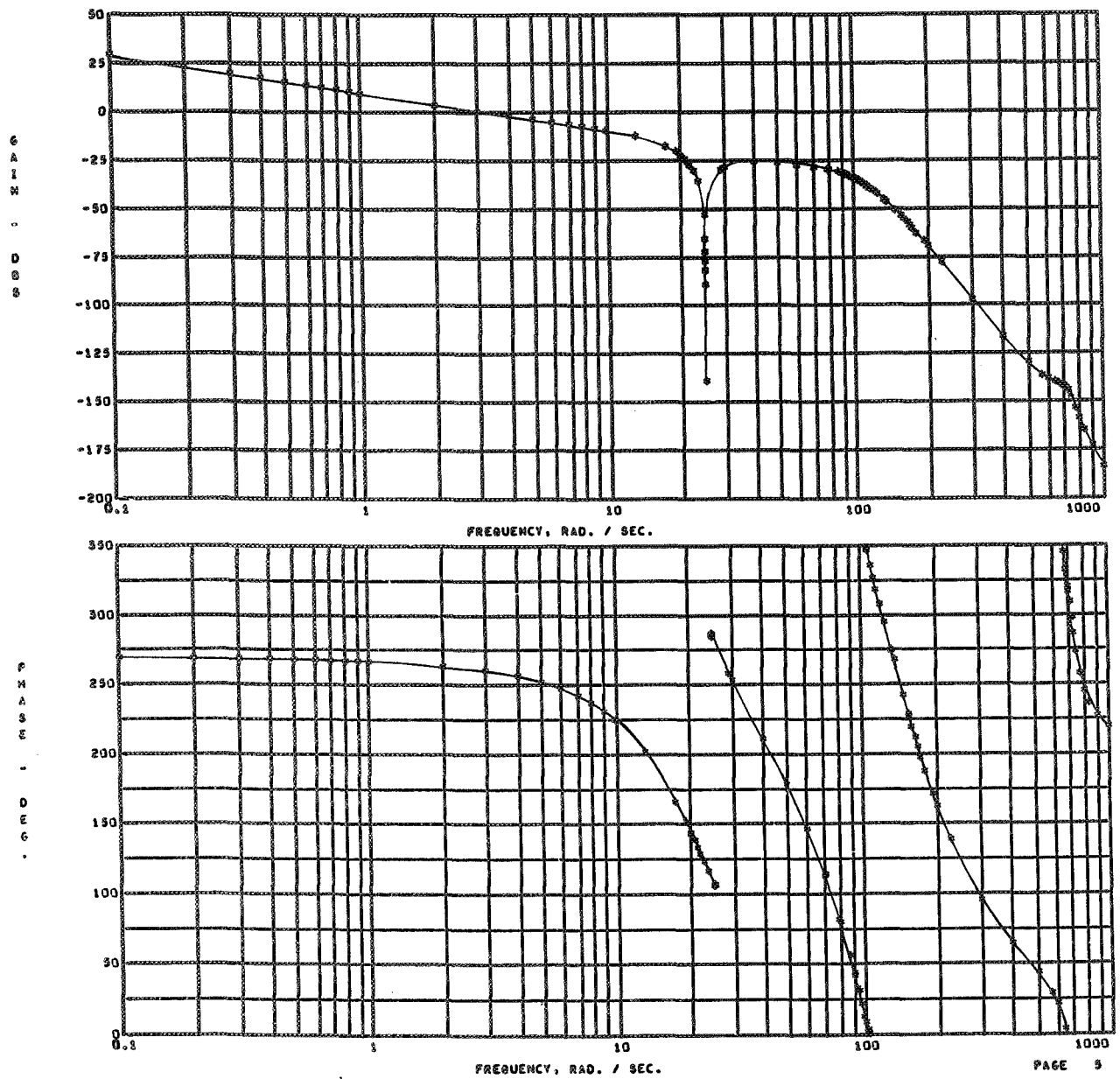


Figure 14

Frequency Response
SCS Rate Loop Open
 $(\psi R/s_c) - K_A = 1/2 \text{ Nom}$

00000000

BODE PLOT

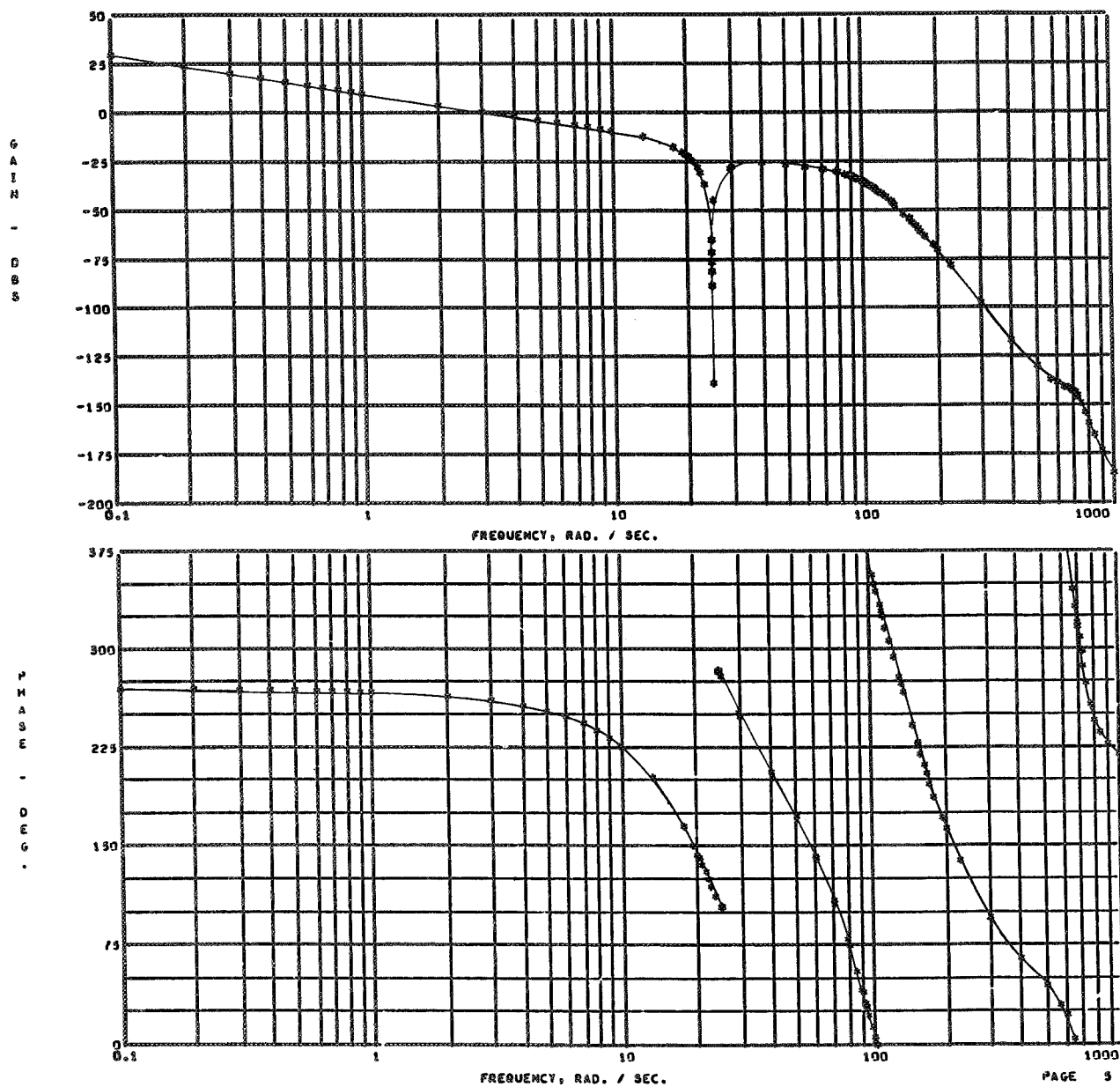


Figure 15

Frequency Response
SCS Rate Loop Open
(ψ_R/δ_C)-All: 1/2 Nom

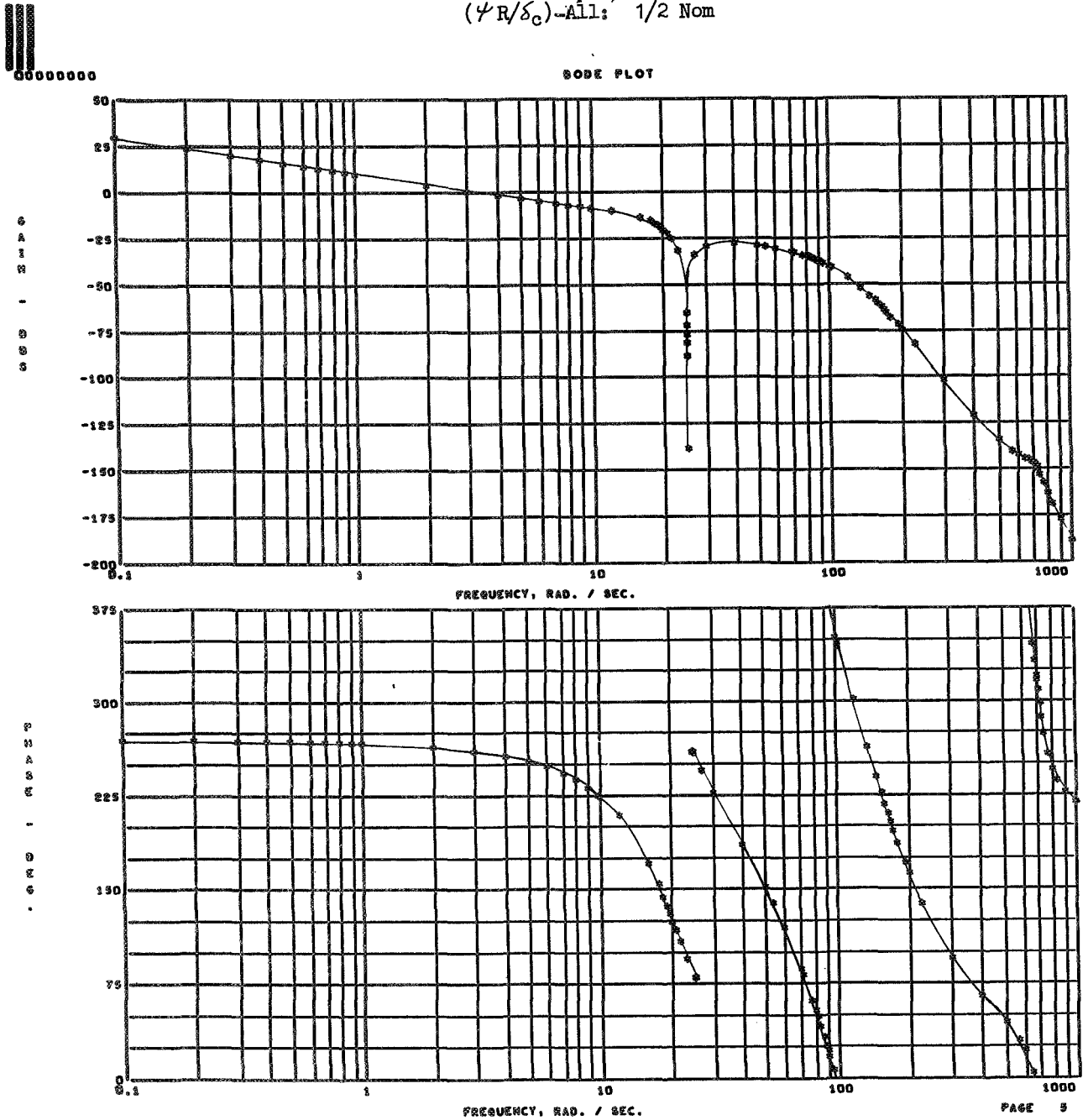
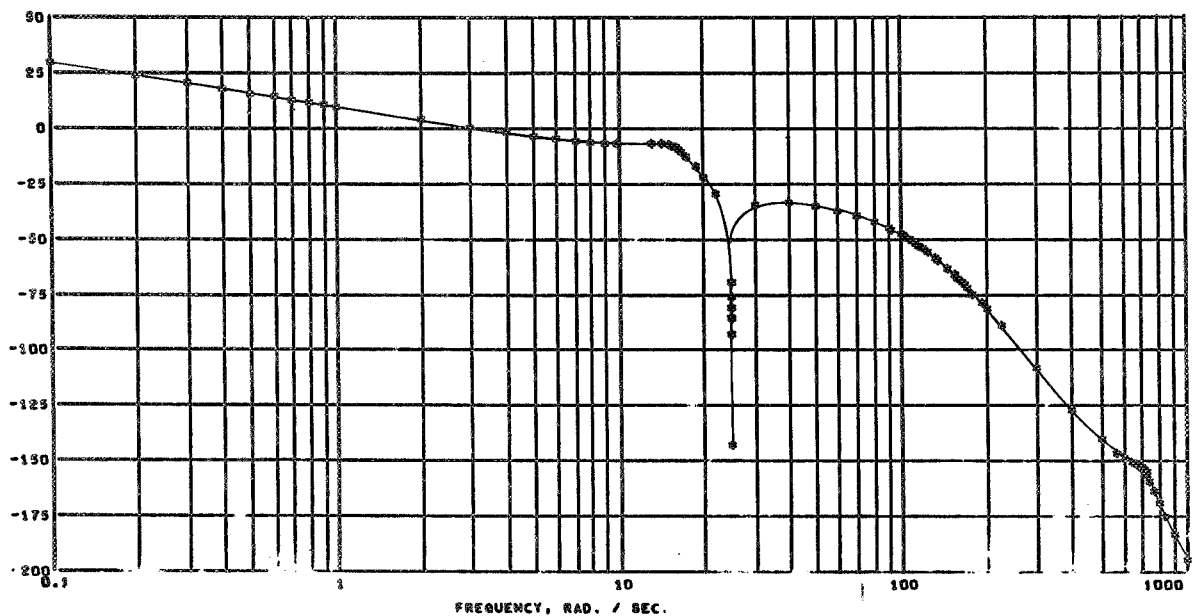
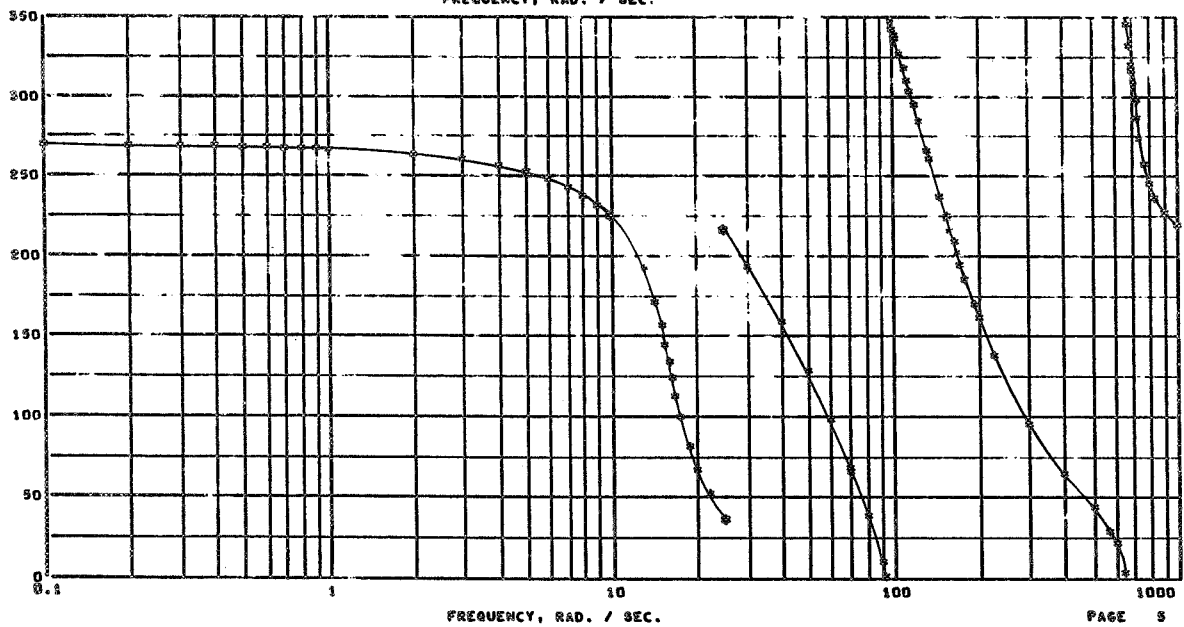


Figure 16

Frequency Response
SCS Rate Loop Open
($\psi R/s_c$) - All: 1/4 Nom

00000000

BODE PLOT

G
A
I
N
-
D
B
SP
H
A
S
E
-
D
E
G

PAGE 5

Figure 17

Frequency Response
 SCS Rate Loop Open
 $(\psi_R/\delta_C) \sim K_T = 2 \text{ Nom}$

00000000

BODE PLOT

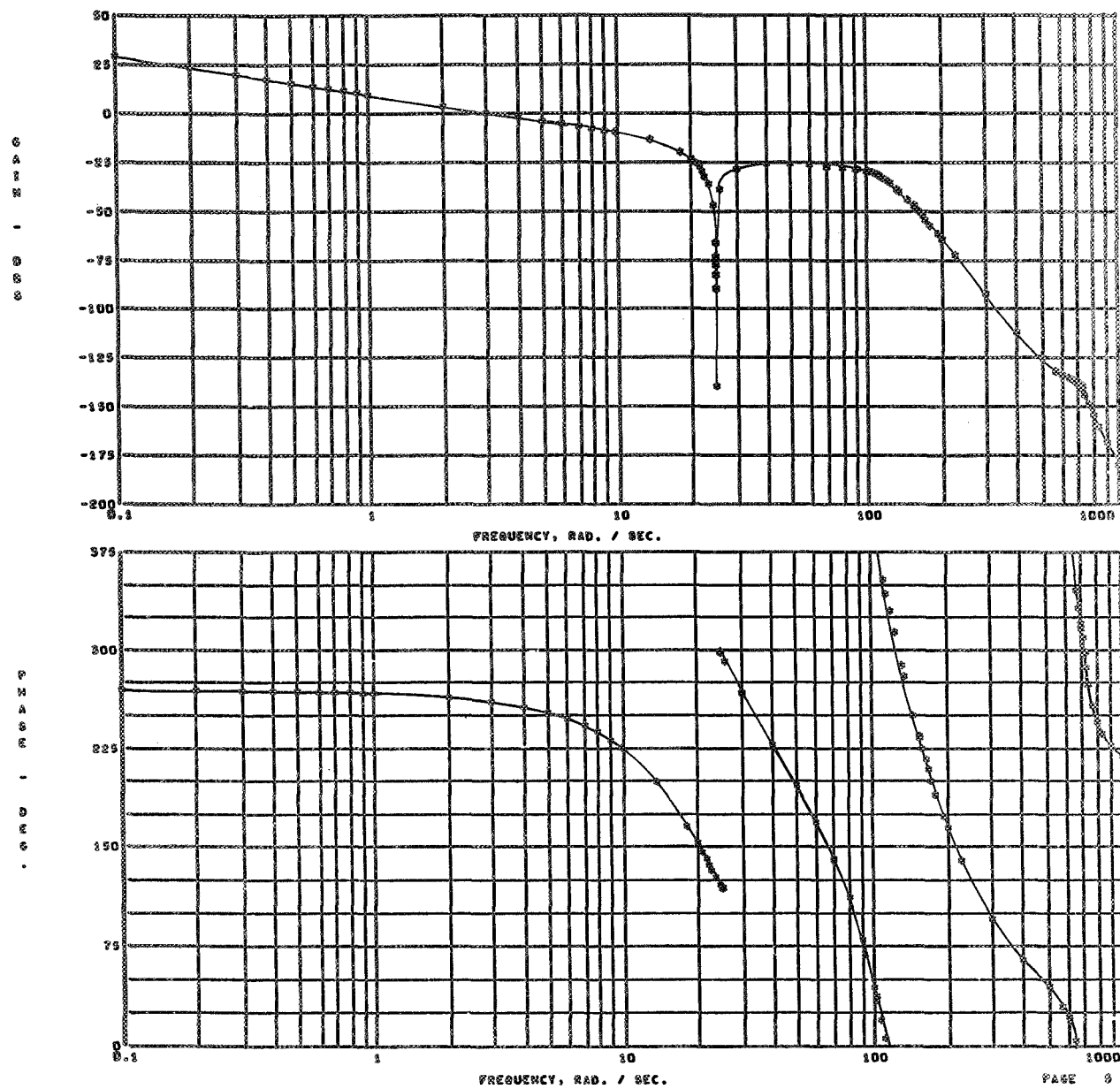


Figure 18

Frequency Response
SCS Rate Loop Open
 $(\psi R/\delta_c) - K_L = 2 \text{ Nom}$



00000000

BODE PLOT

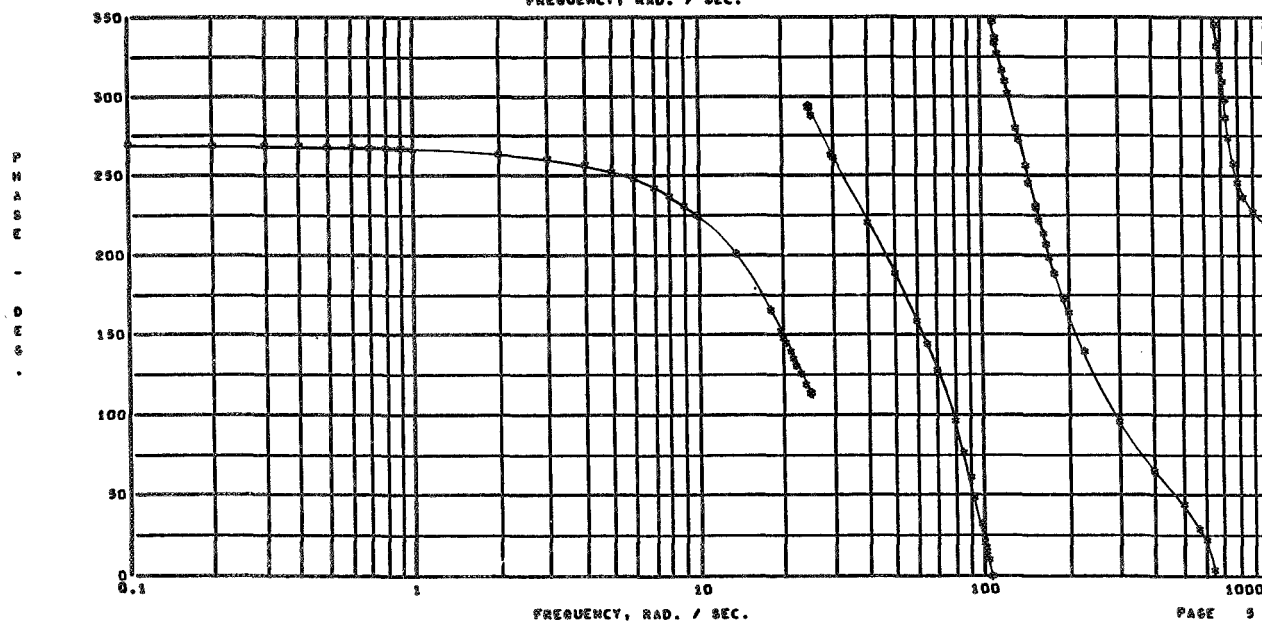
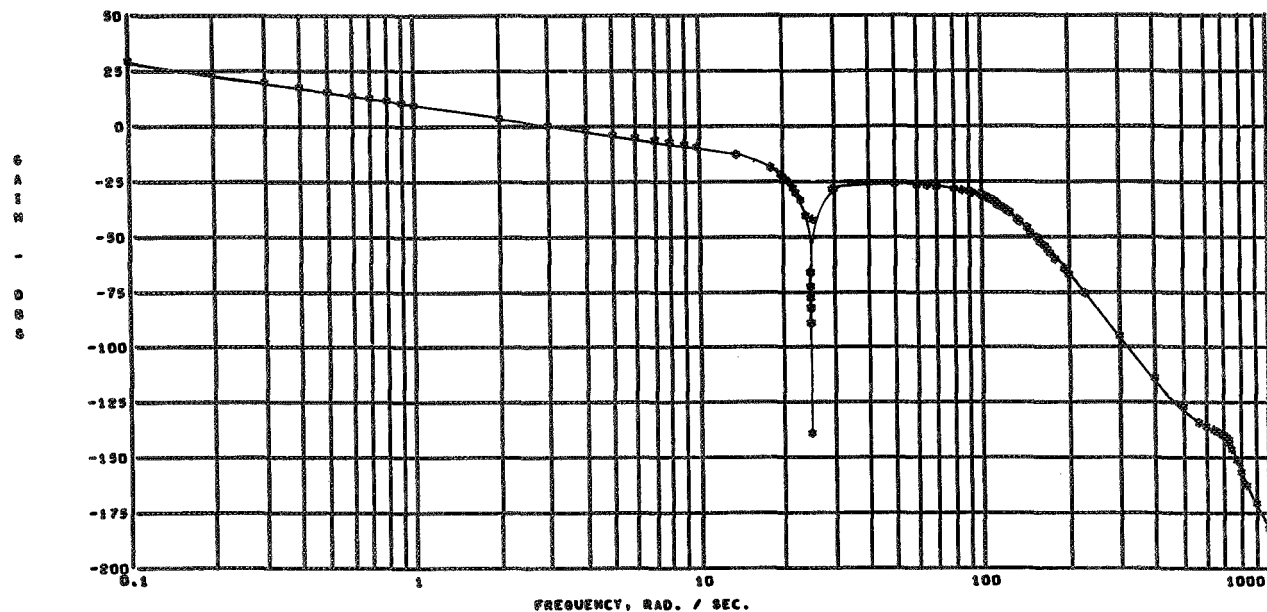


Figure 19

Frequency Response
SCS Rate Loop Open
 $(\psi R/\%_c) - K_A = 2 \text{ Nom}$

00000000

BODE PLOT

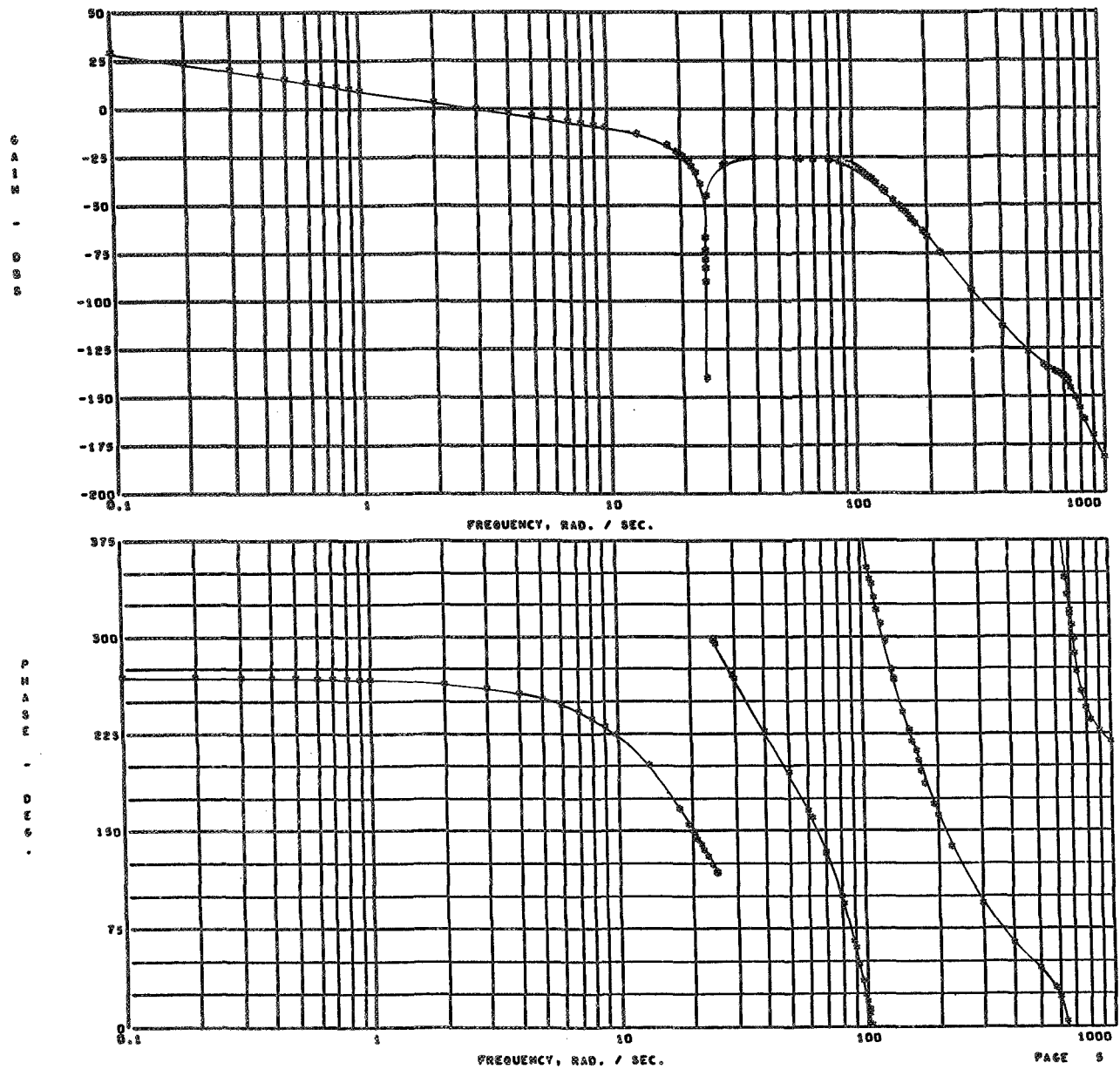


Figure 20

Frequency Response
SCS Position Loop Open
(γ_F/γ_E) - Nominal

00000000

BODE PLOT

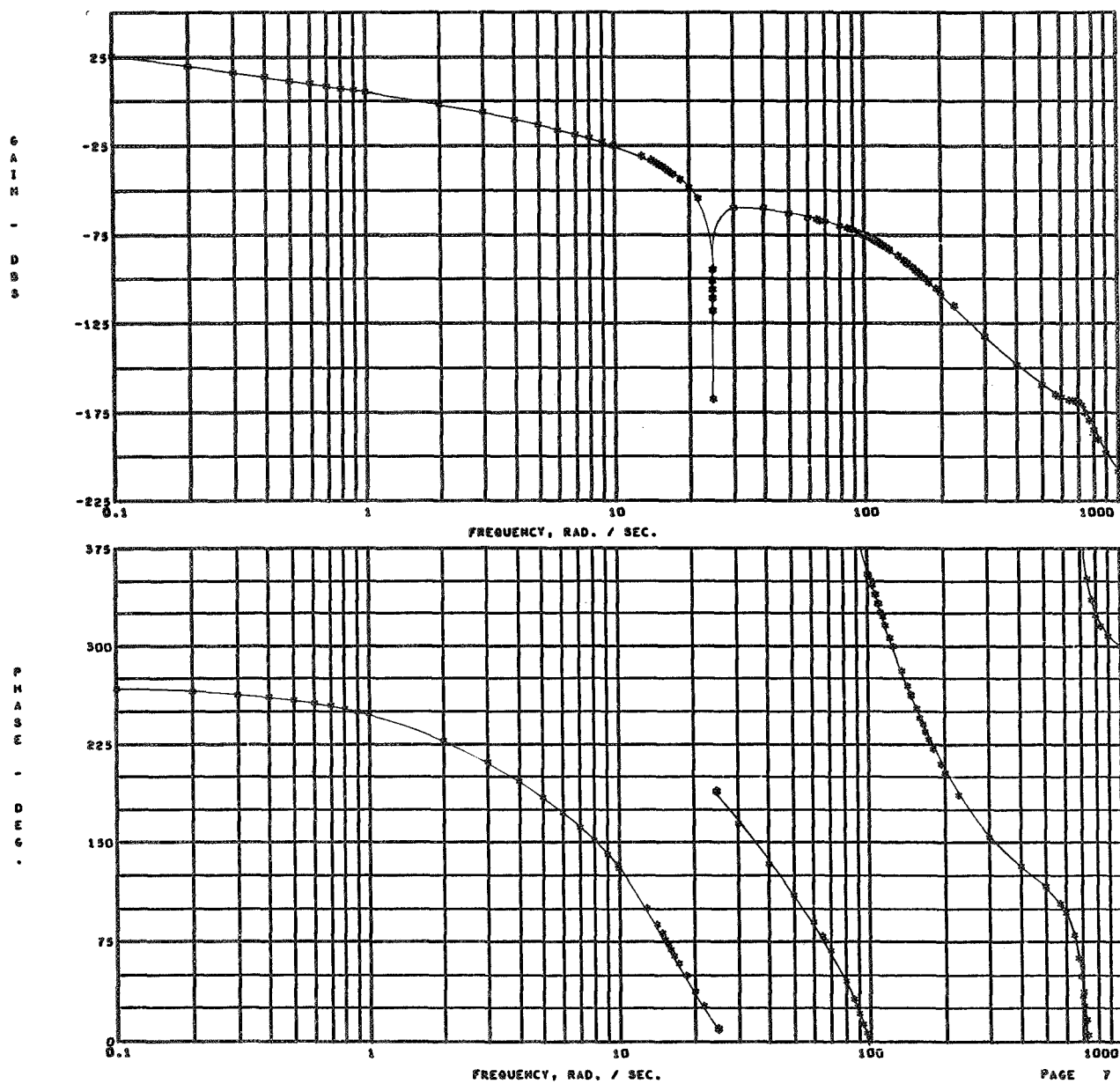


Figure 21

Frequency Response
SCS Position Loop Open
 $(\psi_F/\psi_E) - K_T = 1/2$ Nom



00000000

BODE PLOT

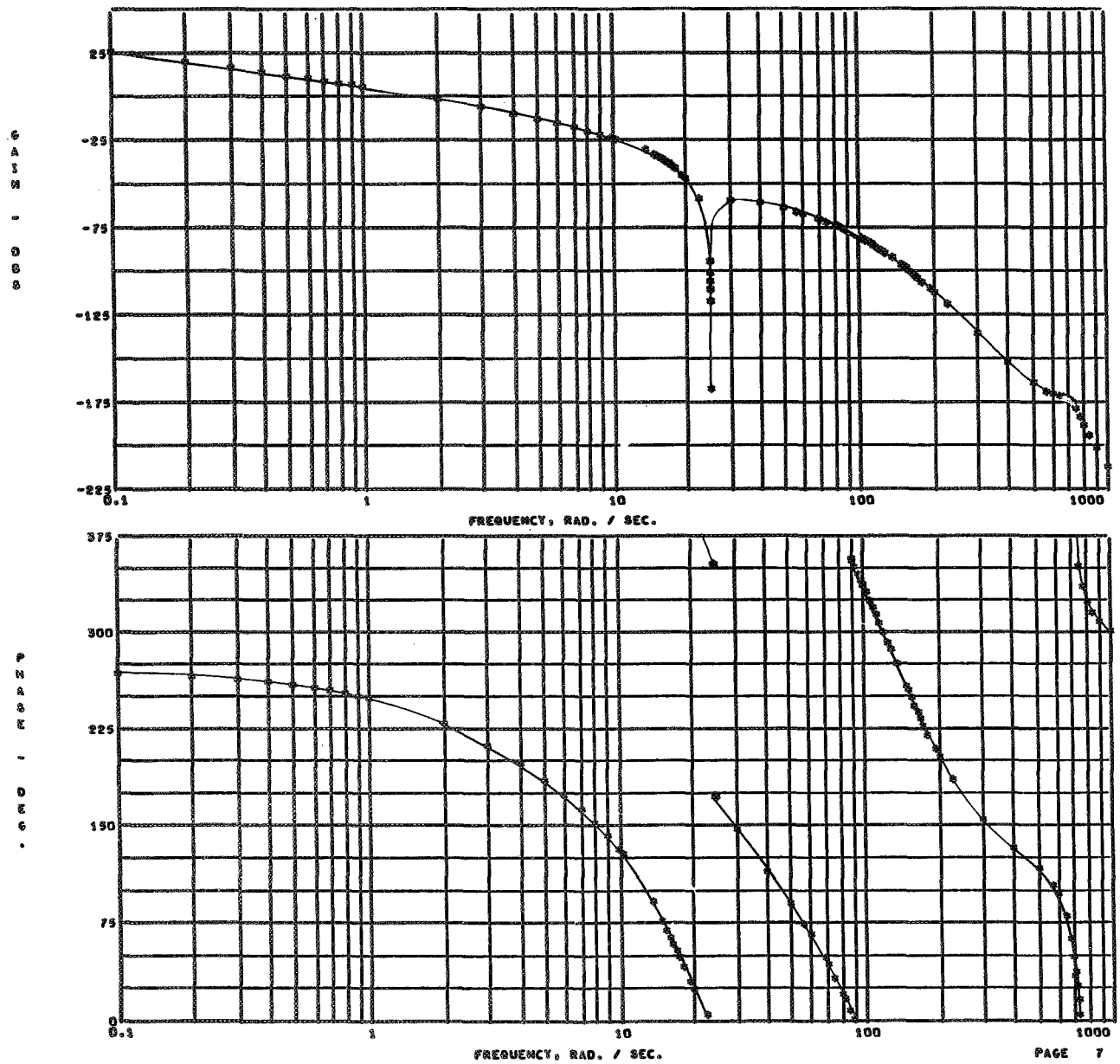


Figure 22

Frequency Response
SCS Position Loop Open
 $(\psi_F/\psi_E) - K_L = 1/2$ Nom

00000000

BODE PLOT

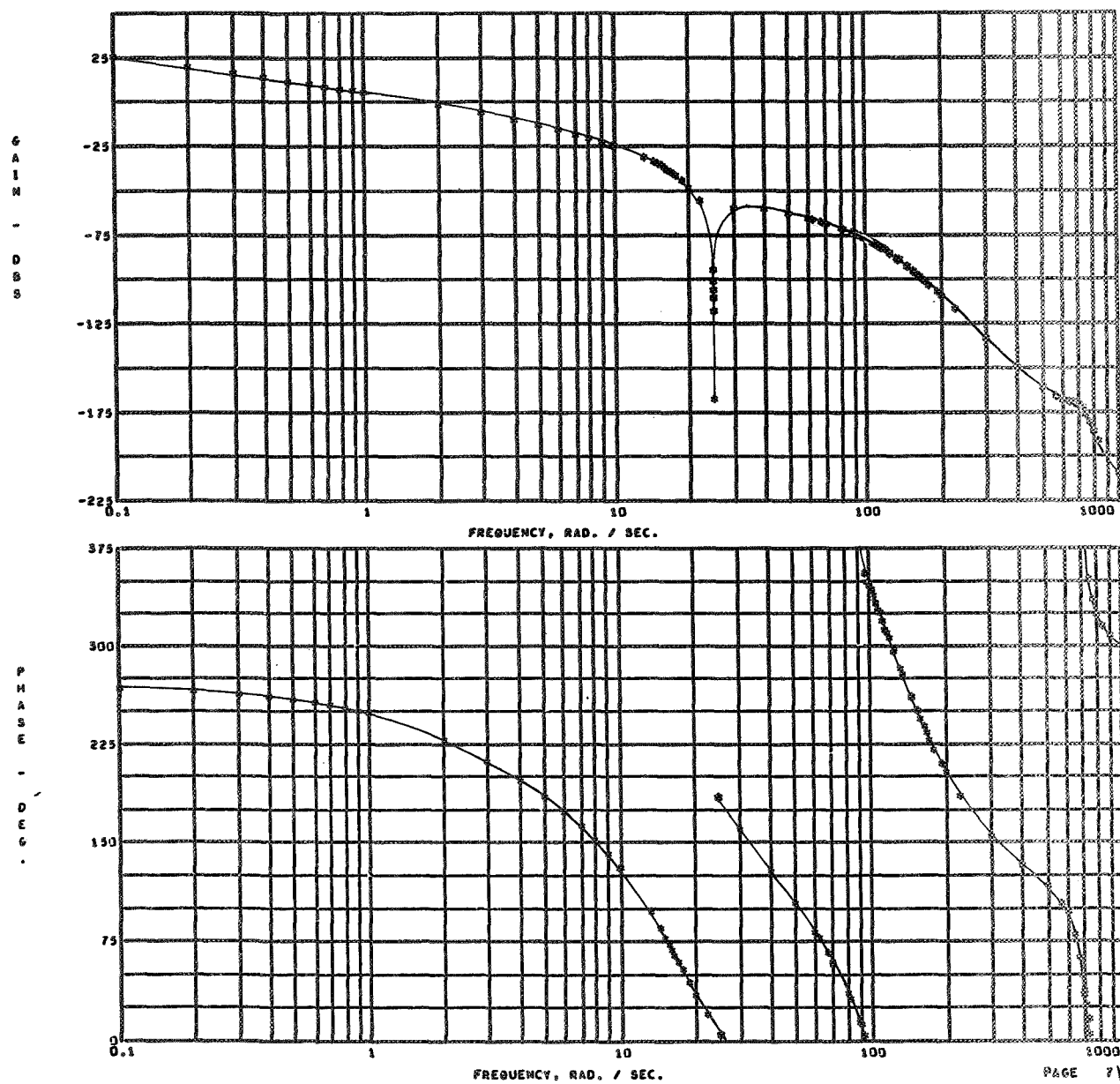


Figure 23

Frequency Response
SCS Position Loop Open
 $(\psi_F/\psi_E) - K_A = 1/2 \text{ Nom}$

00000000

BODE PLOT

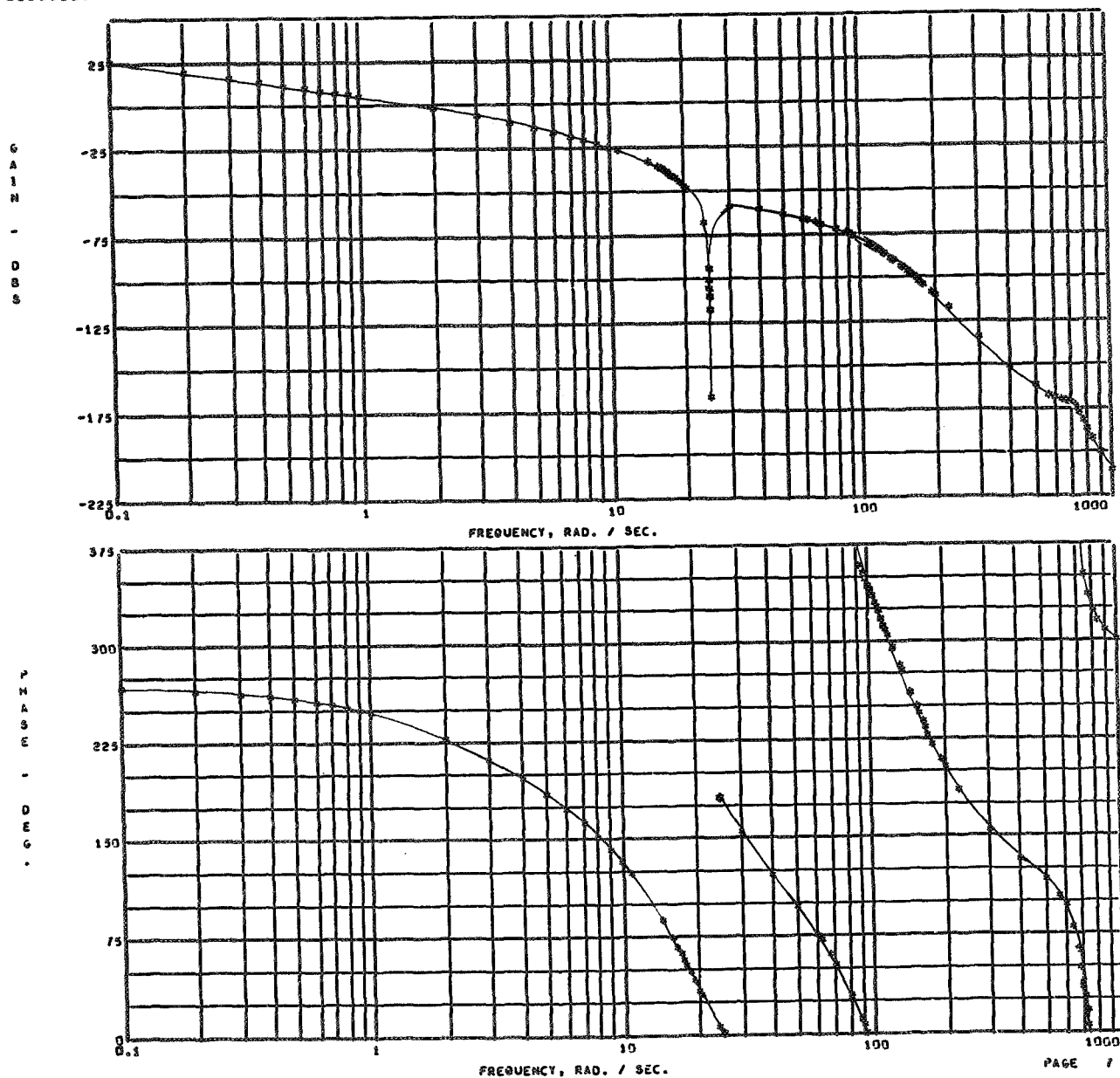


Figure 24

Frequency Response
SCS Position Loop Open
(ψ_F/ψ_e)-All: 1/2 Nom

00000000

BODE PLOT

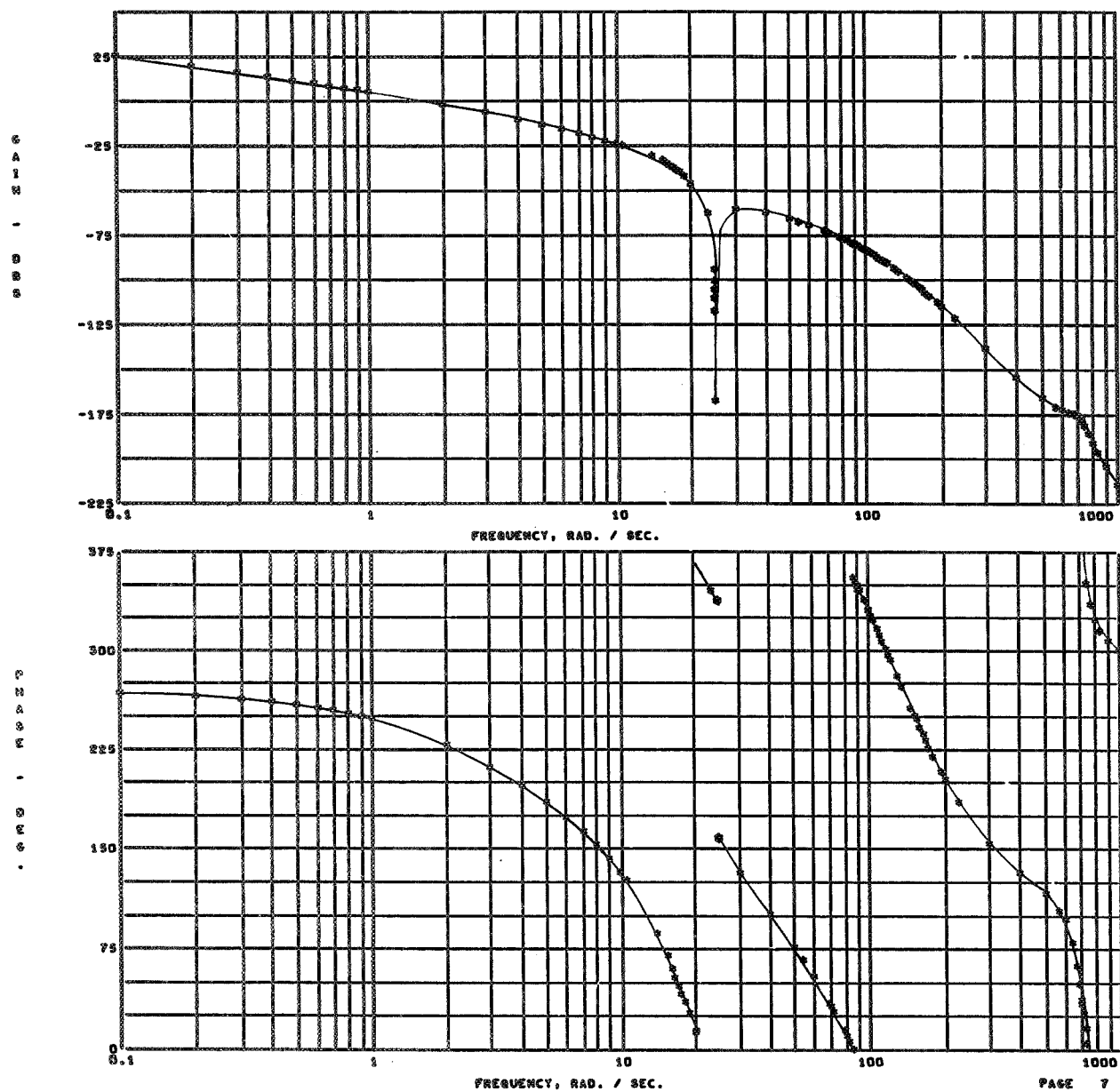


Figure 25

Frequency Response
SCS Position Loop Open
(ψ_F/ψ_E)-All: 1/4 Nom

00000000

BODE PLOT

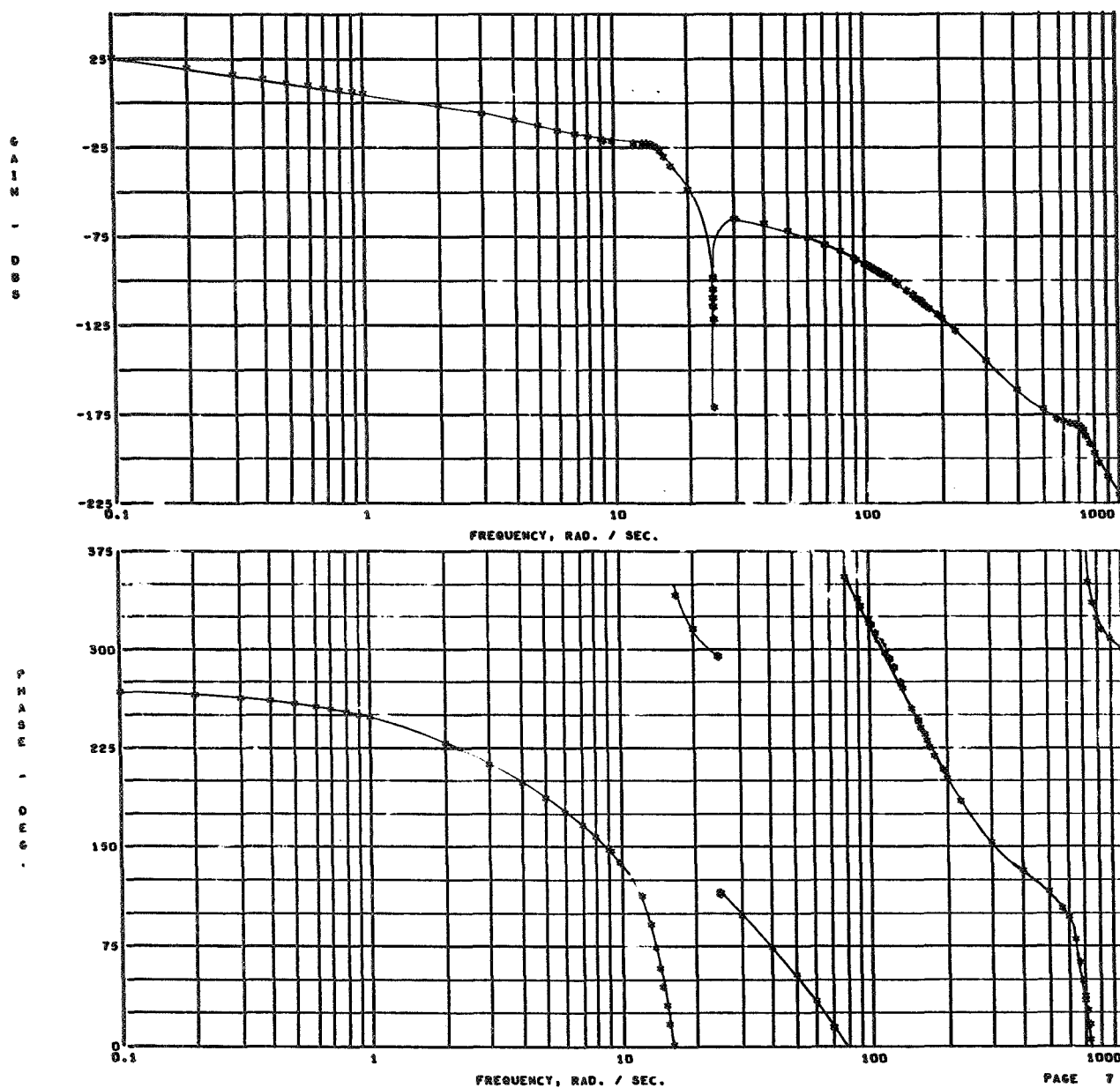


Figure 26

Frequency Response
SCS Position Loop Open
 $(\psi_F/\psi_E) - K_T = 2 \text{ Nom}$

00000000

BOBE PLOT

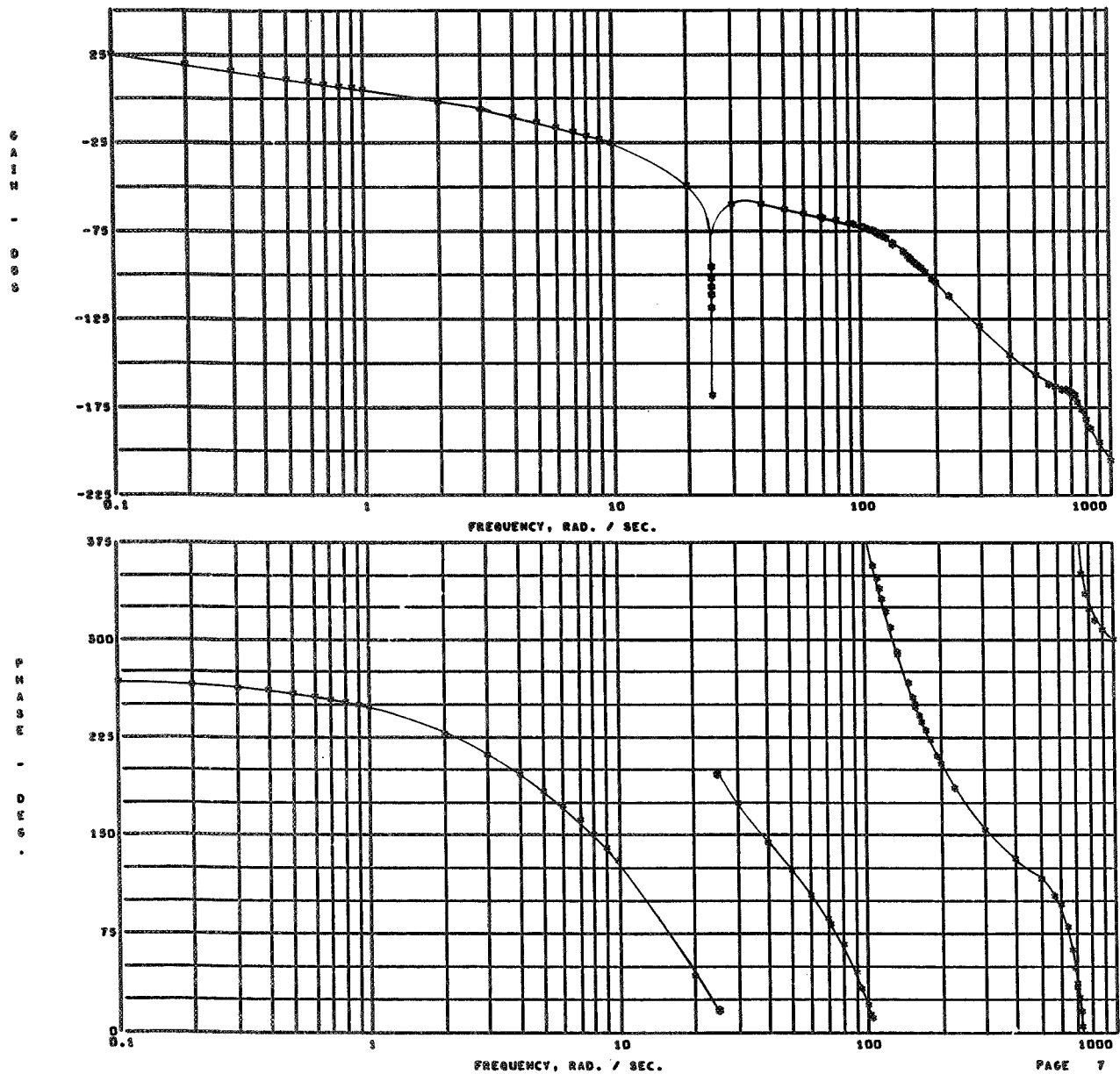


Figure 27

Frequency Response
SCS Position Loop Open
 $(\psi_F/\psi_E) - K_L = 2 \text{ Nom}$

00000000

BODE PLOT

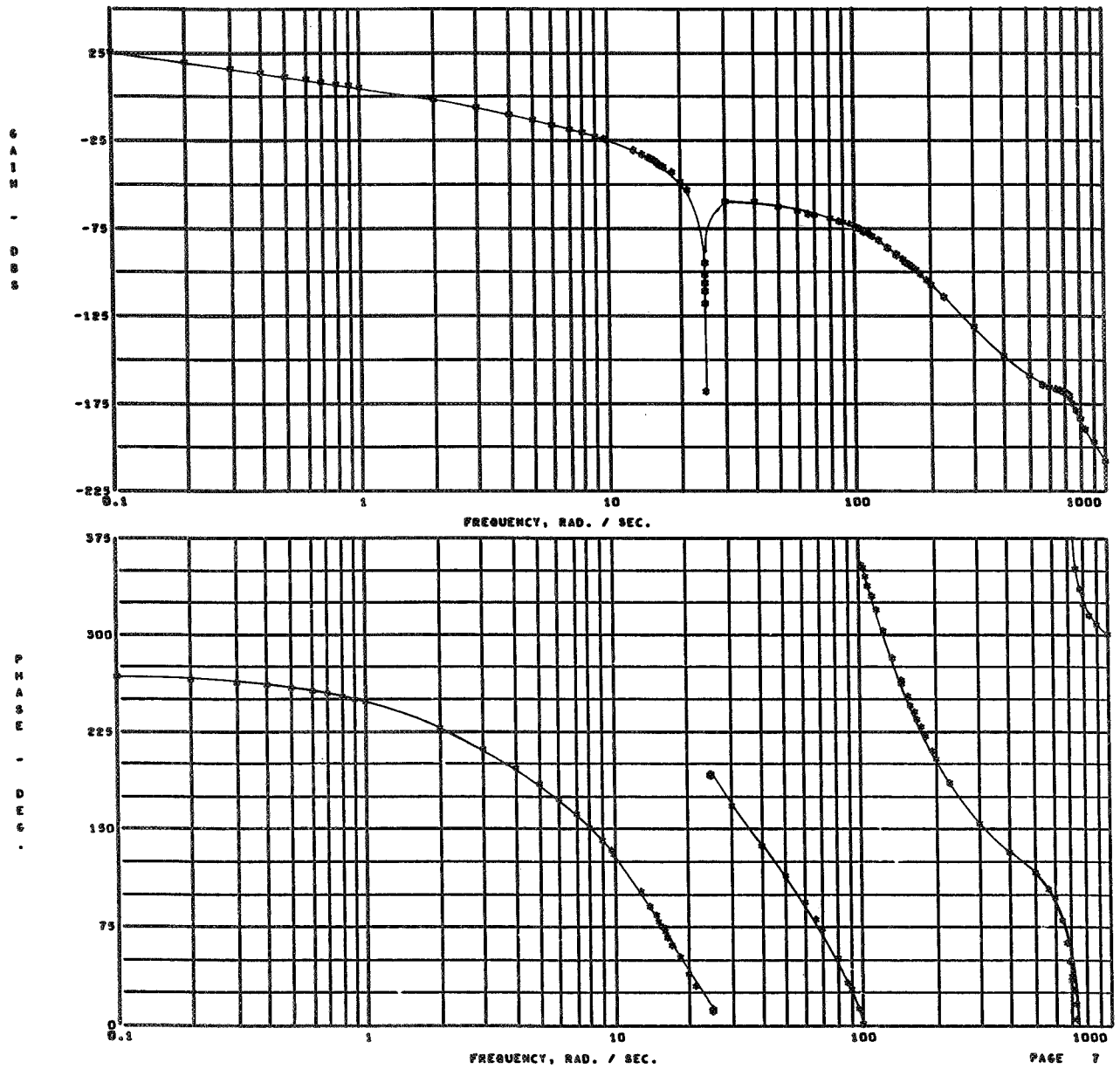


Figure 28

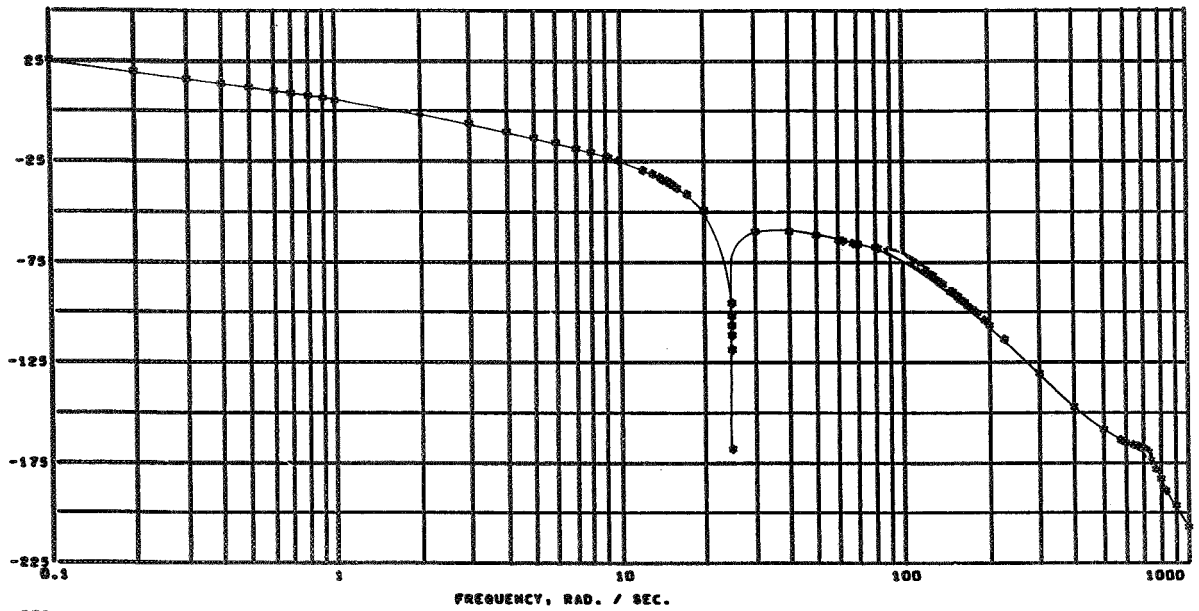
Frequency Response
SCS Position Loop Open
 $(\psi_F/\psi_E)_{-K_A} = 2 \text{ Nom}$



00000000

BODE PLOT

G
A
I
N
-
D
B



P
H
A
S
E
-
D
E
G
.

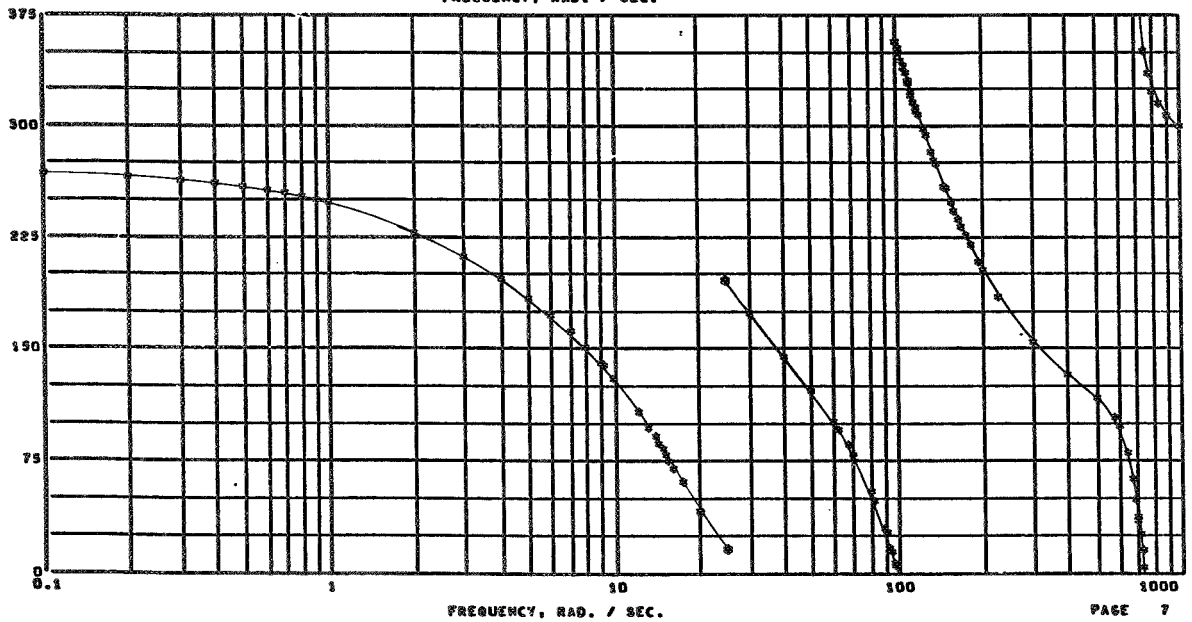


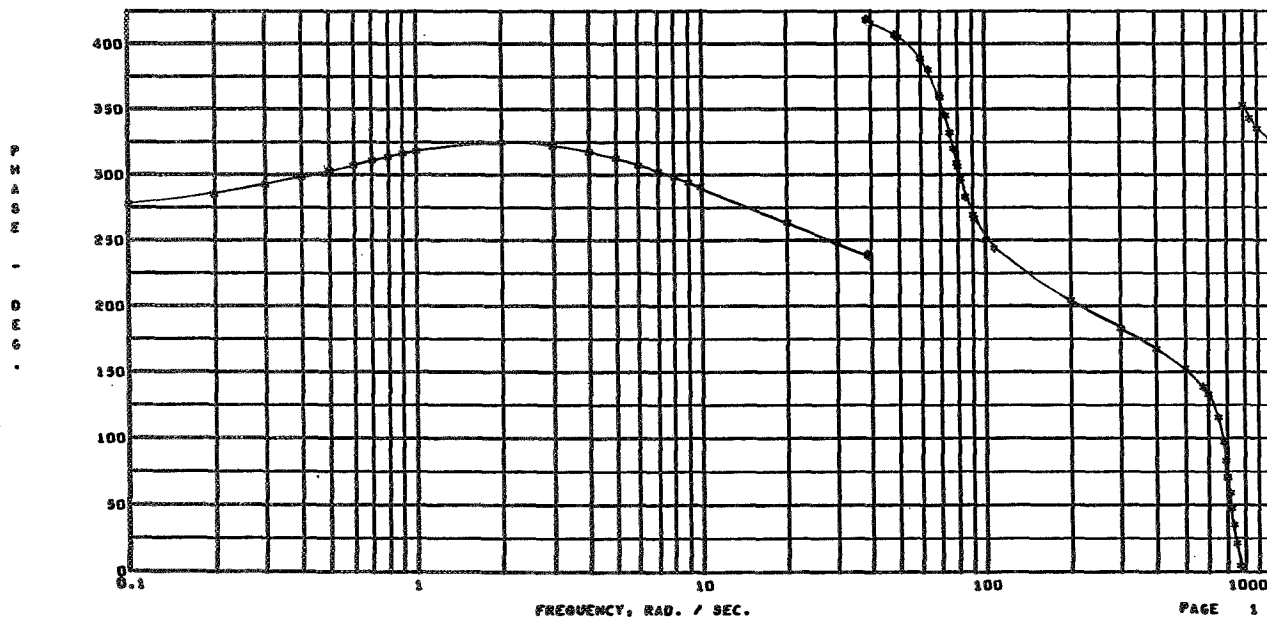
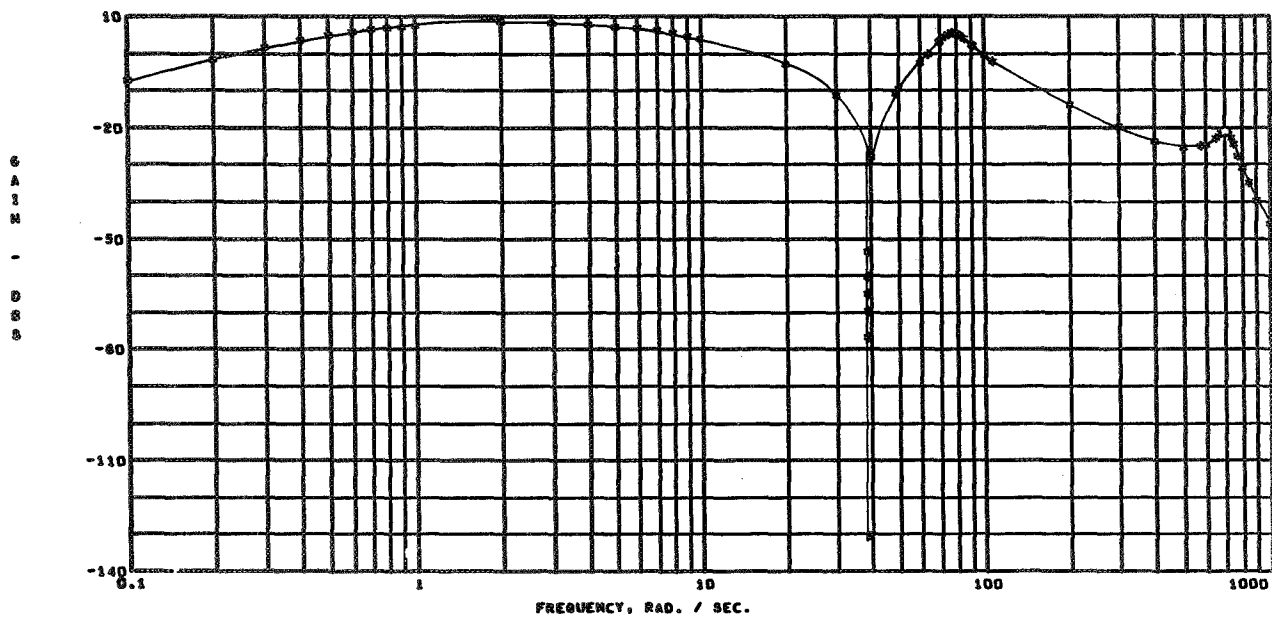
Figure 29

Frequency Response
SPS Rate Loop Open
($\delta R/\epsilon$)—Nominal



00000000

BODE PLOT



PAGE 1

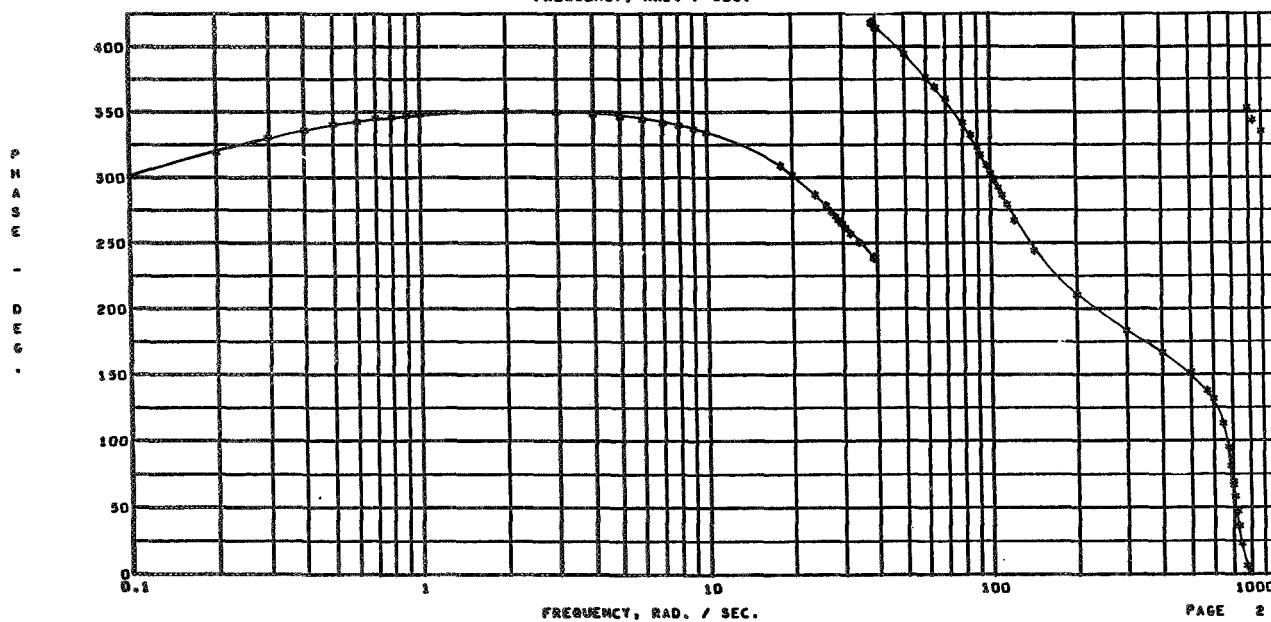
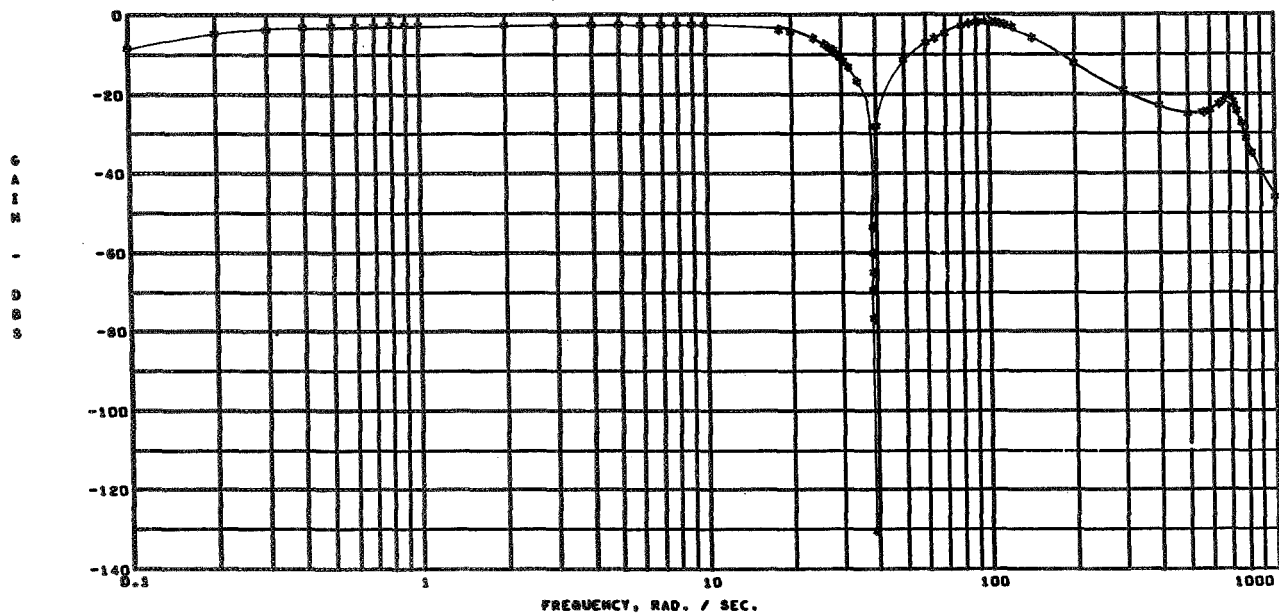
Figure 30

Frequency Response
SPS Rate Loop Closed
($\delta R/\delta \epsilon$)-Nominal



00000000

BODE PLOT



PAGE 2

Figure 31

Frequency Response
SPS Position Loop Closed
($\delta F/\delta_c$)- Nominal

00000000

BODE PLOT

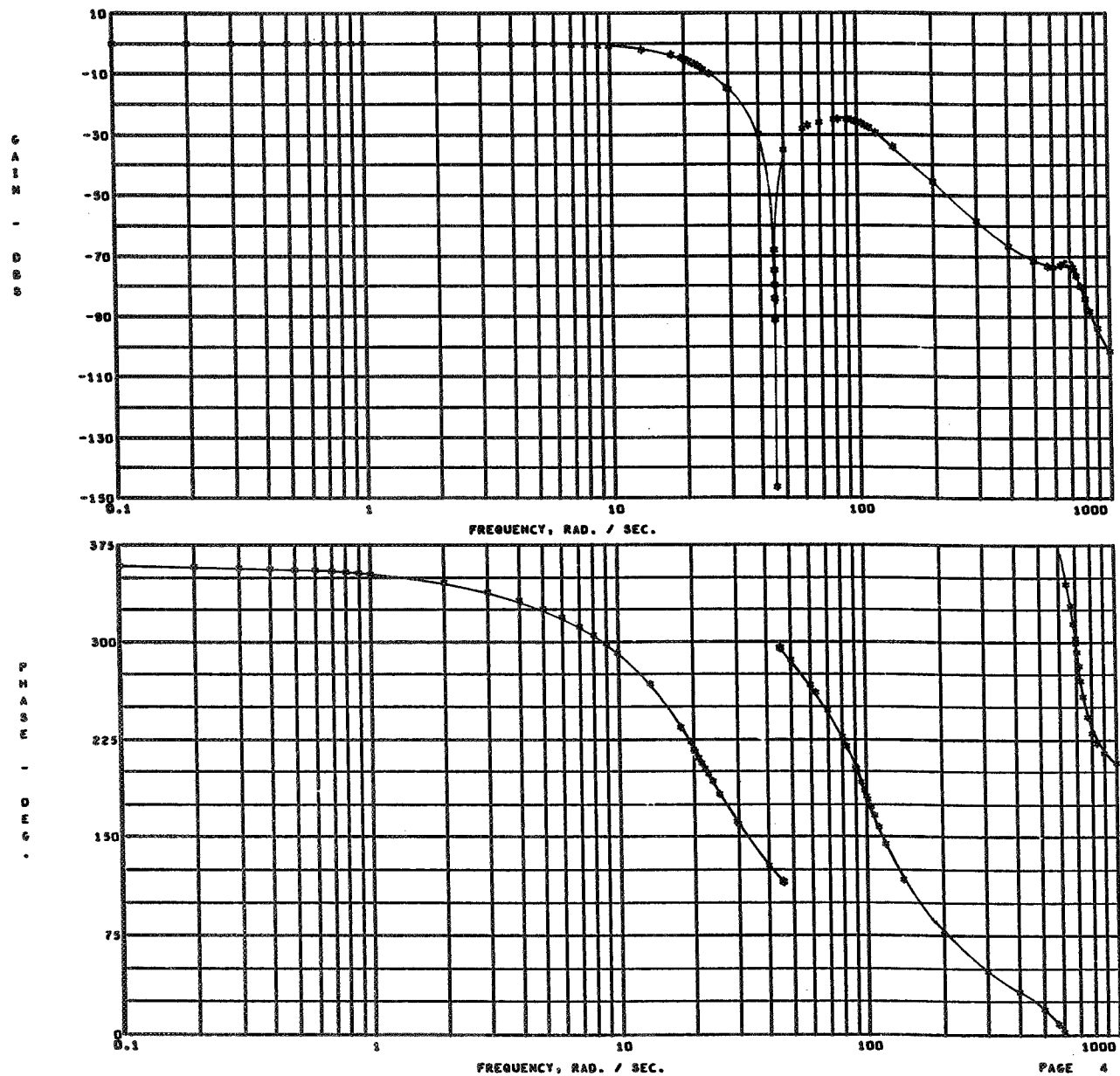


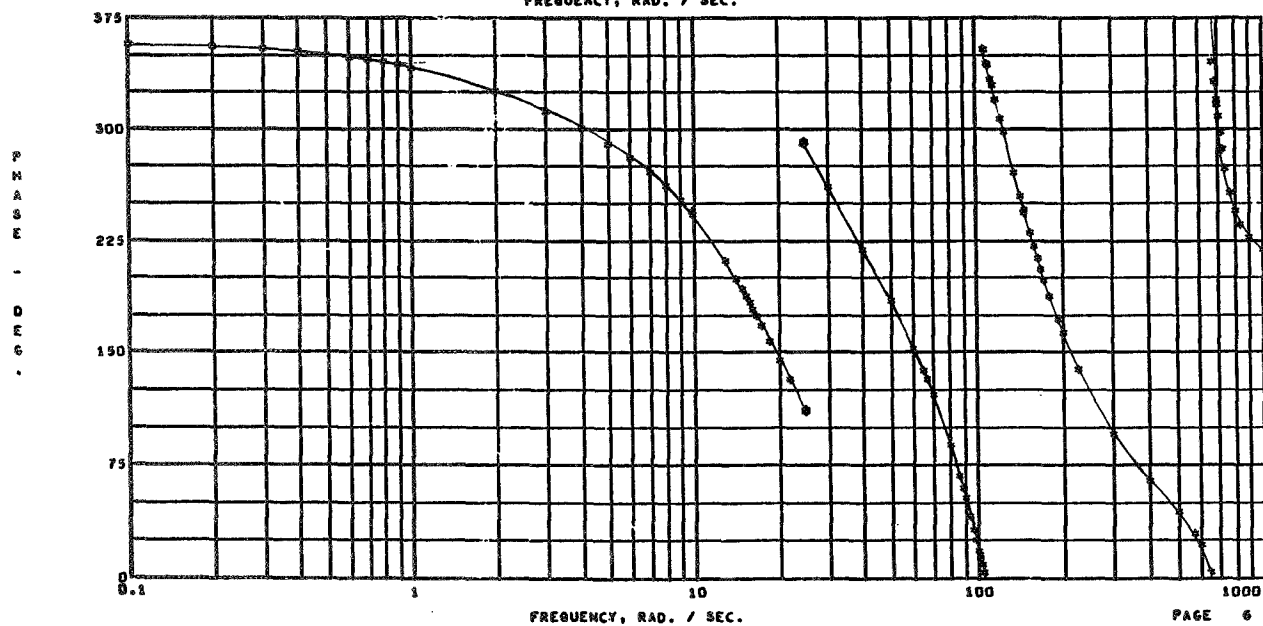
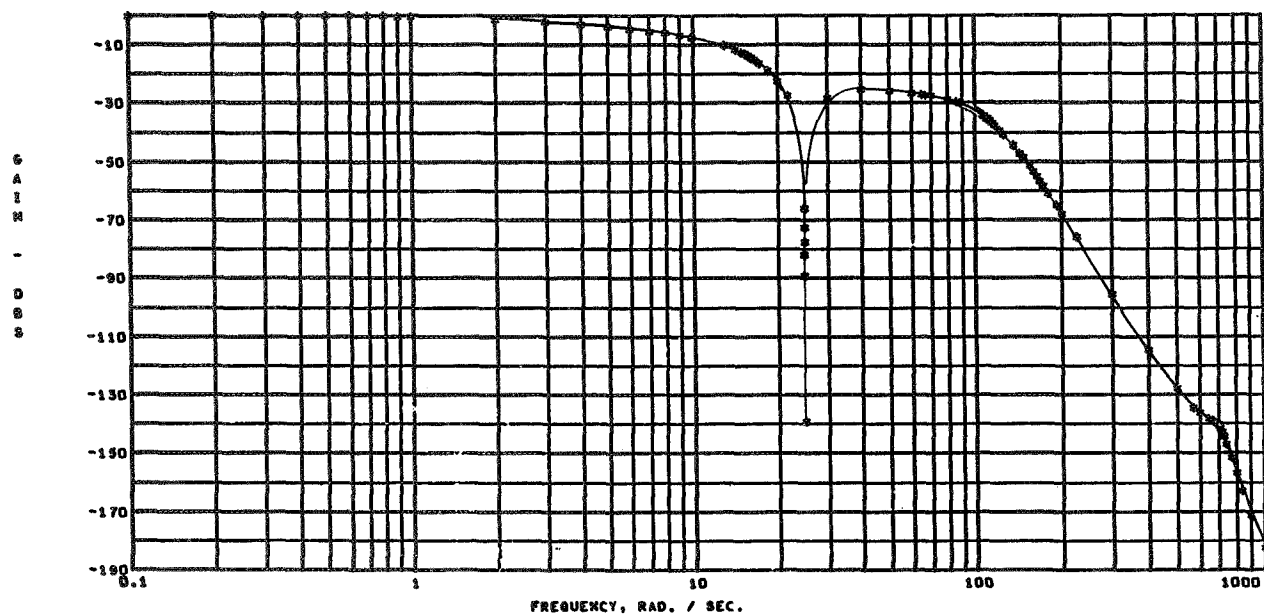
Figure 32

Frequency Response
SCS Rate Loop Closed
(ψ_R/ψ_E)-Nominal



00000000

BODE PLOT



PAGE 6

Figure 33

Frequency Response
SCS Position Loop Closed
(ψ_F/ψ_C)-Nominal

00000000

BODE PLOT

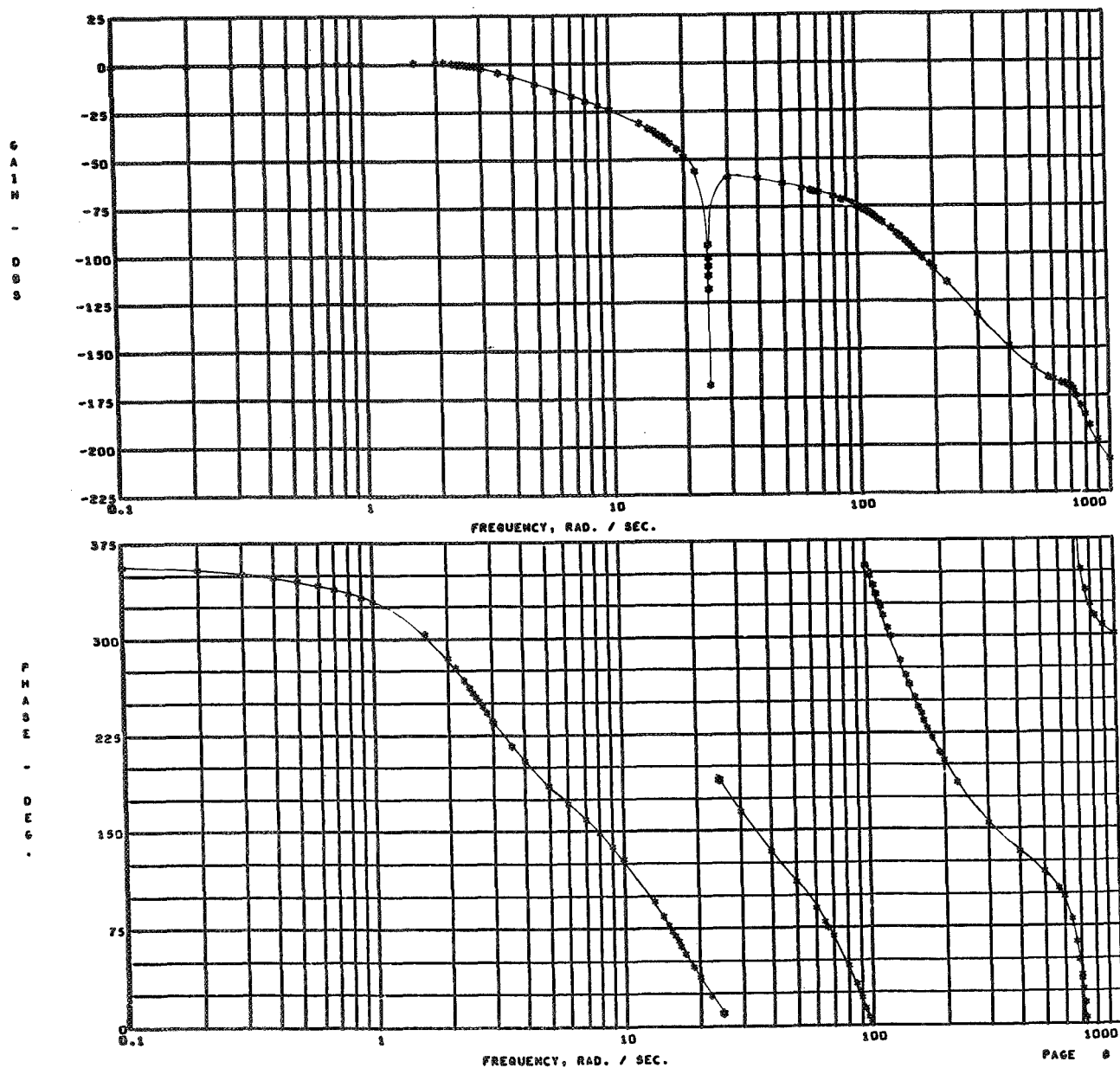


Figure 34

SAS
CLOSED LOOP POLES*
FIGURE 35

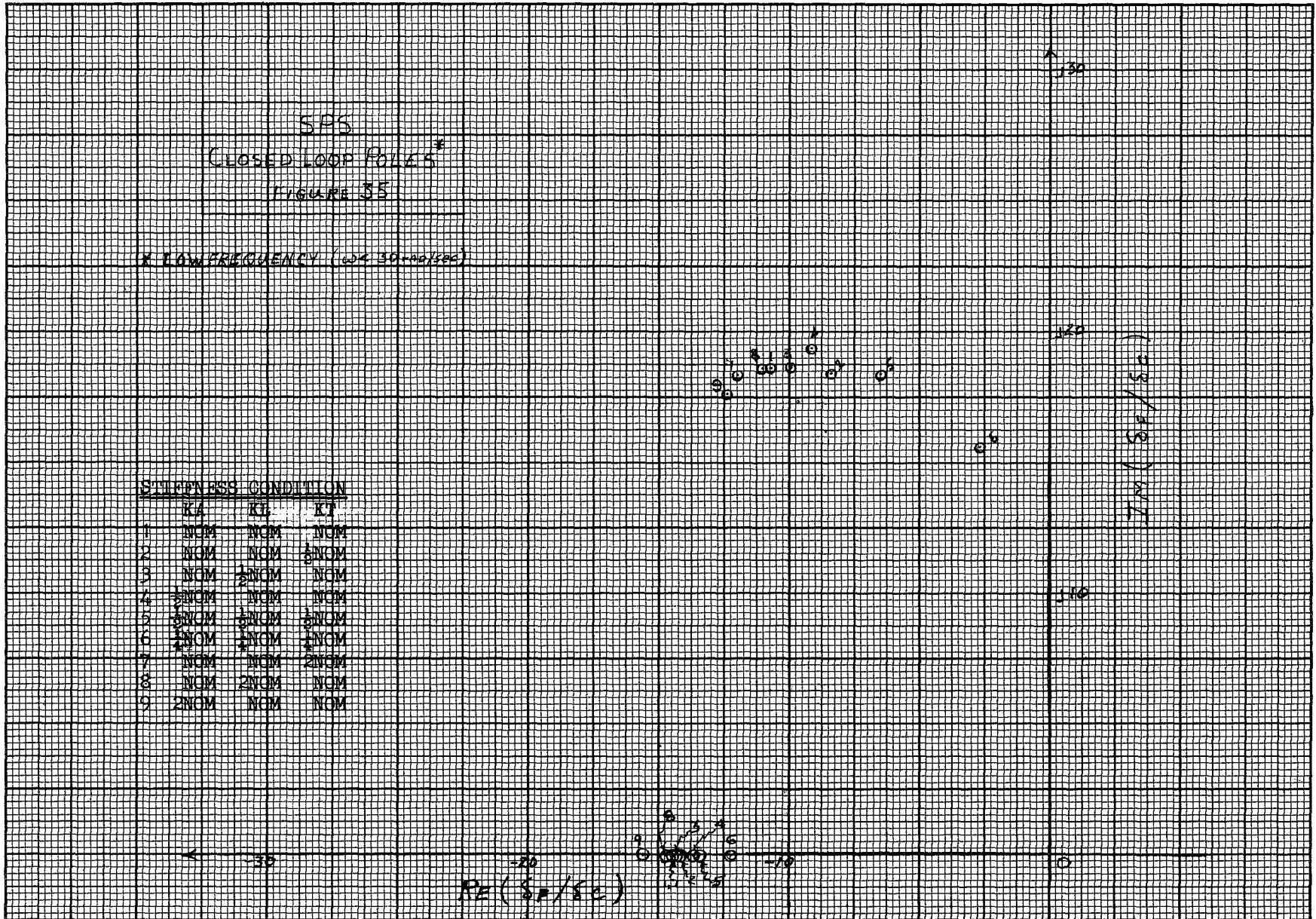
* LOW FREQUENCY ($\omega < 30 \text{ rad/sec}$)

STEPPINESS CONDITION

	K_A	K_E	K_T
1	NOM	NOM	NOM
2	NOM	NOM	$\frac{1}{2}$ NOM
3	NOM	$\frac{1}{2}$ NOM	NOM
4	$\frac{1}{2}$ NOM	NOM	NOM
5	$\frac{1}{2}$ NOM	$\frac{1}{2}$ NOM	$\frac{1}{2}$ NOM
6	$\frac{1}{2}$ NOM	$\frac{1}{2}$ NOM	$\frac{1}{2}$ NOM
7	NOM	NOM	2NOM
8	NOM	2NOM	NOM
9	2NOM	NOM	NOM

$Re(s_p/s_c)$

$Im(s_p/s_c)$



SCS
ATTITUDE RATE LOOP
CLOSED LOOP POLES
FIGURE 36

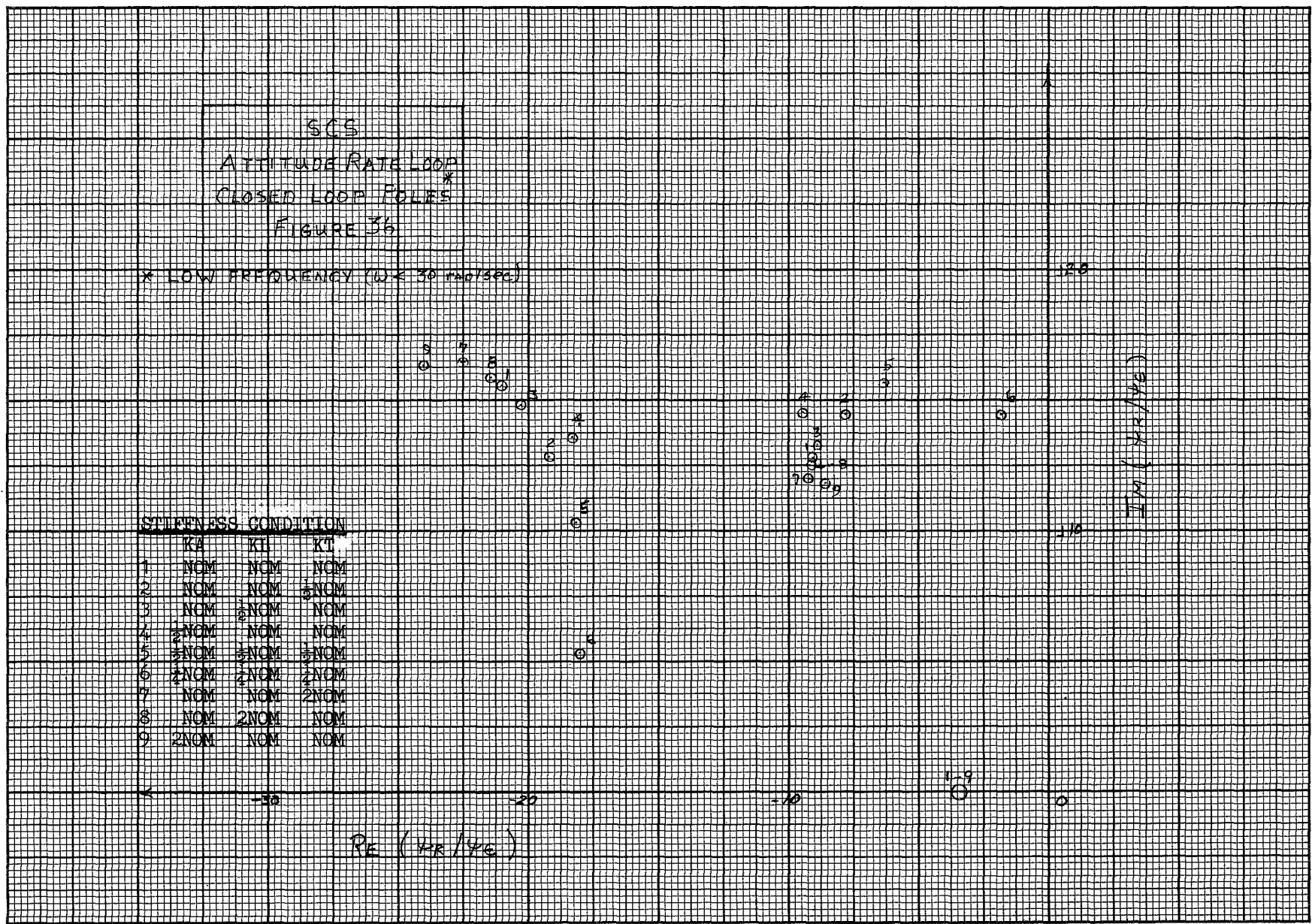
* LOW FREQUENCY ($\omega \ll 30 \text{ rad/sec}$)

STIFFNESS CONDITION

	K_A	K_I	K_T
1	NOM	NOM	NOM
2	NOM	NOM	2NOM
3	NOM	2NOM	NOM
4	2NOM	NOM	NOM
5	2NOM	2NOM	2NOM
6	2NOM	2NOM	2NOM
7	NOM	NOM	2NOM
8	NOM	2NOM	NOM
9	2NOM	NOM	NOM

RE (HR/YG)

IM (HR/YG)



SCS
ATTITUDE POSITION LOOP
CLOSED LOOP POLES*
FIGURE 37

* LOW FREQUENCY ($\omega < 30 \text{ rad/sec}$)

STIFFNESS CONDITION

	K_A	K_I	K_T
1	NOM	NOM	NOM
2	NOM	NOM	$\frac{1}{2}$ NOM
3	NOM	$\frac{1}{2}$ NOM	NOM
4	$\frac{1}{2}$ NOM	NOM	NOM
5	$\frac{1}{2}$ NOM	$\frac{1}{2}$ NOM	$\frac{1}{2}$ NOM
6	$\frac{1}{2}$ NOM	$\frac{1}{2}$ NOM	$\frac{1}{2}$ NOM
7	NOM	NOM	2 NOM
8	NOM	2 NOM	NOM
9	2 NOM	NOM	NOM

